

L-469

ARR No. 3L10

NATIONAL ADVISORY COMMITTEE FOR AERONAUTICS

WARTIME REPORT

ORIGINALLY ISSUED
December 1943 as
Advance Restricted Report 3L10

WIND-TUNNEL INVESTIGATION OF AN NACA 23012 AIRFOIL WITH
A 0.30-AIRFOIL-CHORD DOUBLE SLOTTED FLAP

By Paul E. Purser, Jack Fischel, and John M. Riebe

Langley Memorial Aeronautical Laboratory
Langley Field, Va.

TECHNICAL LIBRARY
RESEARCH MANUFACTURING CO.
9351-9951 SEPULVEDA BLVD.
INGLEWOOD,
CALIFORNIA

MAR 21 1947



WASHINGTON

NACA WARTIME REPORTS are reprints of papers originally issued to provide rapid distribution of advance research results to an authorized group requiring them for the war effort. They were previously held under a security status but are now unclassified. Some of these reports were not technically edited. All have been reproduced without change in order to expedite general distribution.

NATIONAL ADVISORY COMMITTEE FOR AERONAUTICS

ADVANCE RESTRICTED REPORT

WIND-TUNNEL INVESTIGATION OF AN NACA 23012 AIRFOIL WITH
A 0.30-AIRFOIL-CHORD DOUBLE SLOTTED FLAP

By Paul E. Purser, Jack Fischel, and John M. Riebe

SUMMARY

Tests to determine the effect of flap position and deflection on the aerodynamic characteristics of an NACA 23012 airfoil with a double slotted flap having a chord 30 percent of the airfoil chord (0.30c) were conducted in the LMAL 7- by 10-foot tunnel. In addition, a few tests were made to determine the aerodynamic section characteristics as affected by the size and shape of the fore flap, by movement of the fore flap and rear flap as a unit, and by variation in the airfoil lower lip. Contours of rear-flap-nose position for various values of maximum section lift coefficient, section profile-drag coefficient, and section pitching-moment coefficient are presented at three selected fore-flap positions for various rear-flap deflections. The complete aerodynamic section characteristics are given at the three selected fore-flap positions for the optimum-lift and optimum-drag positions of the rear flap at several deflections. Polars of the section profile-drag coefficient at the flap positions and deflections for optimum lift and optimum drag are shown. A discussion is given of the relative merits of the present arrangement as compared with a 0.2566c and a 0.40c slotted flap, a 0.30c Fowler flap, and a 0.40c double slotted flap on the same airfoil.

The optimum deflection of the rear flap within the range investigated at each position of the 0.117c fore flap was 60° in almost all cases and the maximum lift of the airfoil was obtained with the fore flap deflected 25° in the rearmost of the three selected positions. The use of the 0.1467c fore flap provided a slightly higher maximum section lift coefficient than was obtained with the smaller fore flap. The 0.30c double slotted flap (0.117c fore flap) gave a maximum section lift coefficient (3.30) that was higher than that of the 0.2566c or 0.40c single slotted flaps, approximately equal to

that of the 0.30c Fowler flap, but about 0.16 less than that of the 0.40c double slotted flap. The profile-drag coefficients of the 0.30c double slotted flap were higher than those of the 0.30c Fowler and the 0.40c double slotted flaps over the entire lift range and higher than those of the two single slotted flaps in the range of section lift coefficients below 2.7. The negative section pitching-moment coefficients at maximum section lift coefficient produced by the 0.30c double slotted flaps were equal to those of the 0.30c Fowler flap and were greater than those produced by other slotted flaps on the same airfoil.

INTRODUCTION

An extensive investigation of various high-lift devices has been undertaken by the NACA to furnish information applicable to the aerodynamic design of wing-flap combinations for improved safety and performance of airplanes. A high-lift device capable of producing high lift with variable drag for landing and high lift with low drag for take-off and initial climb is believed to be desirable. Other desirable characteristics are: no increase in drag with the flap neutral, small change in pitching moment with flap deflection, low forces required to operate the flap, and freedom from possible hazard due to icing.

Aerodynamic data on the NACA 23012 airfoil have been made available for single slotted flaps in references 1 and 2, for a Fowler flap having a chord 30 percent of the airfoil chord (0.30c) in reference 3, and for a 0.40c double slotted flap in reference 4.

The data presented in reference 4 indicated that the double slotted flap gave higher lift than the single slotted flap and had lower drag at high section lift coefficients. The double slotted flap also had higher lift than the Fowler flap.

Although an investigation essentially the same as that reported herein had been planned at LMAL several years ago, no tests were made at that time because of other projects of greater interest. Renewed interest of designers and manufacturers in devices capable of

L-469
producing very high lift on combat airplanes, however, led to the present investigation, in which tests were made of a 0.30c double slotted flap on the NACA 23012 airfoil (fig. 1). It was believed that this device would combine the advantageous aerodynamic characteristics of the 0.40c double slotted flap (reference 4) with the structural advantages of the small single slotted flap (reference 1). The small size of the fore flap would also allow the use of simpler doors for sealing the break in the airfoil lower surface with the flaps retracted.

APPARATUS AND TESTS

Models

The basic airfoil used in these tests had a chord of 3 feet and a span of 7 feet. The model was constructed of laminated pine and was built to the NACA 23012 profile; the ordinates for the section are presented in table I. This airfoil had previously been used for the investigations reported in references 1, 2, and 4. The trailing-edge section of the model ahead of the flap was equipped with lips of steel plate rolled to the airfoil contour and extending back to the flap in order to provide the basic airfoil contour when the flap was retracted (fig. 1).

The double slotted flap consisted of a fore flap and a rear flap. Two fore flaps (A and B) were used in this investigation. The larger one designated fore flap B was used in only a few tests to determine the effect of increased thickness and chord. The two fore flaps were of different profile, as shown in figure 2, and were built to the ordinates given in table I. Fore flap A was constructed of laminated wood and had a trailing-edge of 1/16-inch steel plate. Fore flap B had an upper surface and trailing-edge of dural and a lower surface of laminated wood.

The rear flap (0.2566c) tested was the one used in the investigations reported in references 1 and 4. The rear-flap profile is shown in figure 1 and the ordinates are given in table I.

Both the fore flap and the rear flap were attached to the main portion of the airfoil by special fittings

that permitted them to be moved and deflected independently. Both the fore flap and the rear flap also pivoted about their respective nose points at any position; increments of 5° deflection were allowed for the fore flap and increments of 10° deflection for the rear flap. The nose point of either flap is defined as the point of tangency of the leading-edge arc and a line drawn perpendicular to the flap chord. The deflection of either flap was measured between its respective chord and the chord of the main airfoil.

The models were made to a tolerance of ± 0.015 inch.

Tests

The model was so mounted in the closed test section of the LMAL 7- by 10-foot tunnel as to completely span the jet except for small clearances at each end. (See references 1 and 5.) The main airfoil was rigidly attached to the balance frame by torque tubes that extended through the upper and lower boundaries of the tunnel. The angle of attack of the model was set by rotating the torque tubes with a calibrated drive from outside the tunnel. This type of installation closely approximates two-dimensional flow and the section characteristics of the model being tested can therefore be determined.

A dynamic pressure of 16.37 pounds per square foot was maintained for all the tests. This dynamic pressure corresponds to a velocity of about 80 miles per hour under standard atmospheric conditions and to an average test Reynolds number of approximately 2,190,000. Because of the turbulence in the wind tunnel, the effective Reynolds number R_e (reference 6) was approximately 3,500,000. For all tests, R_e is based on the chord of the airfoil with the flaps retracted and on a turbulence factor of 1.6 for the wind tunnel.

No tests were made of the plain airfoil nor of the model with the double slotted flap completely retracted because the characteristics of the plain airfoil had previously been investigated and reported in reference 1.

Because of the large number of tests involved in determining the optimum positions of the double slotted flap, a preliminary survey was made to determine the

optimum final position and deflection of fore flap A. Three positions of the fore flap were selected. Positions 1 and 2 were chosen arbitrarily and the deflection for position 2 was the optimum as determined from a survey with the rear flap deflected 40° , 50° , and 60° . Position 3 was the optimum final position and deflection of fore flap A as determined with the rear flap deflected 50° and 60° . Tests were thereafter made at each of these three positions and deflections of the fore flap, as previously determined, to obtain the maximum lift and the optimum position of the rear flap at several deflections. Tests were made with fore flap B at various deflections and positions in the region of the optimum position of fore flap A, and with the rear flap deflected 60° and 70° in the region of its optimum position as determined from tests with fore flap A. In addition, in order to determine the effect on the aerodynamic characteristics, tests were made with the lower lip of the airfoil trailing-edge section in its normal position on the contour, deflected 13.5° within the airfoil contour in order to provide a smoother slot entry, and also completely removed.

An angle-of-attack range from -6° to the angle of attack for maximum lift was covered in 2° increments for each test. No data were obtained for angles of attack above the stall because of the unsteady condition of the model. Lift, drag, and pitching moment were measured at each angle of attack.

RESULTS AND DISCUSSION

Coefficients and Symbols

All the test results are given in standard section nondimensional coefficient form corrected for tunnel-wall effect and turbulence as explained in reference 1.

c_l section lift coefficient (l/qc)

cd_o section profile-drag coefficient (d_o/qc)

$c_m(a.c.)_o$ section pitching-moment coefficient about aerodynamic center of plain airfoil

$$\left[\frac{m(a.c.)_o}{qc^2} \right]$$

$\left[c_{m(a,c)_0} \right]_{c_{l_{\max}}}$ section pitching-moment coefficient
at maximum section lift coefficient

$c_{l_{\max}}$ maximum section lift coefficient

$c_{d_{0\min}}$ minimum section profile-drag coefficient

where

l section lift

d_0 section profile drag

$m(a,c)_0$ section pitching moment about aerodynamic
center of plain airfoil

q dynamic pressure $\left(\frac{1}{2} \rho V^2 \right)$

c chord of basic airfoil with flap fully retracted

V velocity, feet per second

ρ mass density of air

and

R_e effective Reynolds number

l_t distance from aerodynamic center of airfoil
to center of pressure of tail, expressed
in airfoil chords

α_0 angle of attack for infinite aspect ratio

δ_{f_1} fore-flap deflection, measured between
fore-flap chord and airfoil chord

δ_{f_2} rear-flap deflection, measured between rear-
flap chord and airfoil chord

x_1 distance from airfoil upper-surface lip to
fore-flap-nose point, measured parallel
to airfoil chord and positive when fore-
flap-nose point is ahead of lip

| | |
|-------|--|
| y_1 | distance from airfoil upper-surface lip to fore-flap-nose point, measured perpendicular to airfoil chord and positive when fore-flap-nose point is below lip |
| x_2 | distance from fore-flap trailing edge to rear-flap-nose point, measured parallel to airfoil chord and positive when rear-flap-nose point is ahead of fore-flap trailing edge |
| y_2 | distance from fore-flap trailing edge to rear-flap-nose point, measured perpendicular to airfoil chord and positive when rear-flap nose is below fore-flap trailing edge |

Precision

The accuracy of the various measurements is believed to be within the following limits:

| | |
|---|---------|
| α_0 , degrees | ±0.1 |
| $c_{l_{max}}$ | ±0.03 |
| $c_{m(a,c)_0}$ | ±0.003 |
| $c_{d_{0min}}$ | ±0.0003 |
| $c_{d_0}(\alpha_1 = 1.0)$ | ±0.0006 |
| $c_{d_0}(c_l = 2.5)$ | ±0.002 |
| δ_{f_1} and δ_{f_2} , degrees | ±0.2 |
| Flap position | ±0.001c |

No corrections were determined (or applied) for the effect of the airfoil or flap fittings because of the large number of tests required. It is believed that their effect, however, is small and that the relative values of the results would not be appreciably affected.

Plain Airfoil

The complete aerodynamic section characteristics of the plain NACA 23012 airfoil (from reference 1) are presented in figure 3. Inasmuch as these data have previously been discussed (reference 1), no further discussion is considered necessary.

Determination of Optimum Flap Configurations

Maximum lift.— The data presented in figures 4 to 6 represent the results of the maximum-lift investigation with fore flap A at each of the three previously determined positions and with the rear flap deflected and located at points over a considerable area with respect to the fore flap. The results are presented as contours of the position of the rear-flap-nose point at various deflections for given lift coefficients.

Complete maximum lift data for the rear-flap-nose positions with the fore flap in the least extended of the three positions (identified herein as position 1) are given in figure 4, showing the rear flap deflected in 10° increments from 10° to 60° . The contours with the fore flap in the intermediate and extended positions (positions 2 and 3) are given in figures 5 and 6, respectively. Because it is unlikely that small rear-flap deflections would ever be used with these extended fore-flap positions, data for the small rear-flap deflections were not obtained. The figures show that all the contours are closed, except that for $\delta_{f_2} = 10^\circ$ at position 1, which indicates that the contour would close at an impractical rear-flap-nose position.

At each of the fore-flap positions, the rear-flap-nose position for maximum lift becomes more critical with increased flap deflection, particularly when δ_{f_2} is 50° and 60° . With increased flap deflection, the position of the rear-flap nose for maximum lift tends to move forward and upward and the gap between the two flaps is thereby decreased. In the following table are given the values of the maximum section lift coefficient obtained at each fore-flap position and the approximate position of the rear-flap nose with respect to the fore-flap trailing edge.

| Fore-flap position | Position of rear-flap nose | | $c_{l_{max}}$ |
|--------------------|---|--------------------------------------|---------------|
| | Ahead of lip (percent airfoil chord) | Below lip (percent airfoil chord) | |
| 1 | 2 | 3 | 2.74 |
| 2 | 2 | 2 | 3.15 |
| 3 | 2 | 2 | 3.30 |

In almost all cases, the highest value of maximum section lift coefficient for the flap-deflection range investigated was obtained at $\delta f_2 = 60^\circ$.

From the contours of rear-flap-nose position for $c_{l_{max}}$, a designer should be able to determine the best path to be followed by the rear flap at all deflections within the range tested, from a consideration of only maximum section lift coefficient. The range of flap positions covered was believed sufficient to allow for any deviations or compromises from the "best lift" path. Complete aerodynamic section characteristics for the optimum rear-flap-nose position for both lift and drag at each fore-flap deflection and position will be presented subsequently in this report.

Minimum profile drag.— Contours of rear-flap-nose position for values of minimum section profile-drag coefficient at specific section lift coefficients and flap deflections are presented in figures 7 to 9 for the three fore-flap positions. A comparison of the contour of figure 7(a) with the section profile-drag characteristics of the plain airfoil (fig. 3) indicates that the plain airfoil gives the lower drag at section lift coefficients of 1.5 or less.

At position 1, the contours of c_{d_0} are presented only for values of δf_2 of 10° , 20° , and 30° , since it is believed that the larger flap deflections at this position would not be used because the corresponding c_{d_0} values are quite high. Inasmuch as all the contours at each of the three fore-flap positions were not closed about the indicated optimum rear-flap-nose positions, it is apparent that a sufficient range of rear-flap positions was not covered and that the true optimum values may exist at some other positions. The contours also indicate that

more than one region of relatively low drag exists for several rear-flap deflections. As anticipated, the minimum section profile-drag coefficient increased with deflection of the rear flap at any given lift coefficient. At the same lift coefficient and rear-flap deflection, values of profile-drag coefficient became less as the fore flap was extended; for example, at $c_l = 1.5$, $\delta f_2 = 30^\circ$, an optimum value of c_{d_0} of 0.050 was obtained at position 2 as compared to a value of 0.063 at position 1; and at $c_l = 2.5$, $\delta f_2 = 50^\circ$, an optimum value of c_{d_0} of 0.103 was obtained at position 3 as compared to a value of 0.117 at position 2. The optimum rear-flap-nose position moved forward and up, closer to the fore-flap lip as the fore flap was extended and also as the rear flap was deflected.

For all these contours (figs. 7 to 9), in each position of the fore flap at high lift coefficients and flap deflections, a given movement of the rear-flap-nose point caused a greater change in the value of c_{d_0} .

Inasmuch as the rear-flap-nose positions for maximum lift and minimum drag generally do not coincide, a compromise is necessary; therefore, complete aerodynamic section characteristics are presented for both conditions.

Pitching moment.— The contours of rear-flap-nose position for values of $c_m(a.c.)_0$ at specific flap deflections and lift coefficients are presented in figures 10 to 12 for each of the three fore-flap positions. Because the positive increment of lift usually obtained with increased flap deflection has its centroid farther to the rear than does an equal lift increment obtained by increased angle of attack, an increase in the negative pitching moment of the airfoil is anticipated when the flap is deflected. The contours for $c_m(a.c.)_0$ tend, therefore, to close near the region of the rear-flap-nose position for maximum lift, and the positions of the rear-flap nose for maximum lift and maximum pitching moment usually coincide.

The negative section pitching-moment coefficients usually increased with lift coefficient and flap deflection and the change in $c_m(a.c.)_0$ for a given change in

rear-flap-nose position became larger as both these variables increased. At a given lift coefficient, the negative values of $c_{m(a.c.)_0}$ also increased as the fore flap was extended and deflected. It appears desirable therefore to use the minimum flap deflection or extension necessary to obtain a given lift coefficient.

With these contours of rear-flap position for $c_{m(a.c.)_0}$ available (figs. 10 to 12), a designer can determine or anticipate the section pitching-moment coefficients to be encountered within the range of positions and deflections investigated.

Aerodynamic Section Characteristics of Selected Optimum Configurations

The complete aerodynamic section characteristics of the airfoil with the optimum-lift and optimum-drag positions of the rear flap at each flap deflection and at each of the three selected fore-flap positions are presented in figures 13 to 15. These figures indicate that the lift-curve slopes decreased with increased flap deflection. The angle of attack for maximum lift usually decreased with increased flap deflection at each position, but in some instances remained practically constant. It will be noted that the aerodynamic section characteristics for optimum lift for $\delta f_2 = 70^\circ$ are presented only for position 3 (fig. 15(a)). Tests were made at $\delta f_2 = 70^\circ$ in both positions 2 and 3, but insufficient data were obtained to present the characteristics for the optimum rear-flap position for position 2 or the contours for either fore flap position; however, at position 3, from data gathered at $\delta f_2 = 70^\circ$ and other deflections, it is believed that the optimum-lift position of the rear flap was attained. The aerodynamic characteristics are therefore given.

The section pitching-moment coefficients in general increased negatively with the rear-flap deflection and as the fore flap was extended. The slopes of the section pitching-moment curves were negative at low angles of attack and low flap deflections and were usually positive at high angles of attack and high flap deflections. At

high section lift coefficients, lower negative values of $c_{m(a,c.)_0}$ were therefore sometimes obtained with a large flap deflection than with a small one. It will be noted in figures 13 and 14 that at $\delta f_2 = 50^\circ$ and 60° , respectively, the position of the rear flap for maximum lift coincides with that for minimum drag, indicating this position to be best from both considerations. In figures 13(a) and 14(a), the irregularities in the curves indicate that changing flow conditions existed at $\delta f_2 = 60^\circ$.

Increment of maximum Section Lift Coefficient.— The effect of flap deflection on $\Delta c_{l_{max}}$ for each of the three fore flap positions is indicated in figure 16. The increment of maximum section lift coefficient, based on the maximum section lift coefficient of the plain airfoil, increased not only with rear-flap deflection but also as the fore flap was extended and deflected.

The values of $\Delta c_{l_{max}}$ for the optimum-lift rear-flap positions are higher than those for optimum drag except at position 1, $\delta f_2 = 50^\circ$, and position 2, $\delta f_2 = 60^\circ$, where the two values coincide. The maximum increment within the range investigated at each fore-flap position occurred at $\delta f_2 = 60^\circ$, except for the optimum-drag curve of position 1. The maximum increment, which was obtained at position 3, was about 1.75. In position 1 $\Delta c_{l_{max}}$ increased only slightly for rear-flap deflections above 30° , and in position 3, the decrease in $\Delta c_{l_{max}}$ was fairly small between $\delta f_2 = 60^\circ$ and 70° .

Envelope Polar Curves.— The envelope polar curves of section profile-drag coefficient at each of the fore flap positions, obtained from figures 13 to 15, and the envelope polar of the plain airfoil are presented in figure 17. These polars show the lowest section profile-drag coefficient obtainable at a given section lift coefficient for the optimum-lift and optimum-drag flap configurations at each fore-flap position.

For section lift coefficients less than 1.5, the plain airfoil gives the lowest section profile-drag coefficient. Position 3 gives in general the lowest values of c_{d_0} for values of c_l greater than 2.0.

Comparison of Flap Arrangements

A comparison of section profile-drag coefficients for the 0.2566c and the 0.40c slotted flaps (references 1 and 2), the 0.30c Fowler flap (reference 3), and the 0.40c double slotted flap (reference 4) is presented in figure 18 with the two envelope polars of the 0.30c double slotted flap obtained from figure 17. This figure shows that although the maximum section lift coefficient of the 0.30c double slotted flap (3.30) is far better than that obtained with either single slotted flap, it is below the value of 3.46 obtained with the 0.40c double slotted flap and approximately equals the value obtained with the 0.30c Fowler flap. This comparison also shows that the 0.30c double slotted flap had a larger profile drag than any of the other arrangements for section lift coefficients greater than 1.2 and less than 2.7 but had a lower profile drag than either single slotted flap at section lift coefficients higher than 2.7. At all values of section lift coefficient, the 0.30c double slotted flap had larger profile drag than either the 0.30c Fowler or the 0.40c double slotted flap arrangements.

The optimum-drag envelope polar of the 0.30c double slotted flap had values of cd_0 that were somewhat lower than those of the optimum lift polar; this difference in cd_0 amounted to as much as 0.02 at $c_l = 2.9$. At section lift coefficients less than 1.6 and higher than 3.1 the polars for optimum lift and optimum drag, however, almost coincide.

A comparison of the section pitching-moment coefficients at the maximum section lift coefficients for the various flap arrangements previously discussed is given in figure 19. The variation of $[c_m(a.c.)_0]_{c_{l_{max}}}$ with

$c_{l_{max}}$ appears to be dependent upon flap arrangement.

The arrangement reported herein gave higher values of $[c_m(a.c.)_0]_{c_{l_{max}}}$ than any of the slotted flaps but its

values are approximately equal to those of the Fowler arrangement.

The loss of airplane maximum section lift coefficient in trimming the airfoil section pitching-moment coefficient is given by the expression

$$\text{Loss of } c_{l_{\max}} = \frac{[c_{m(a.c.)_0}] c_{l_{\max}}}{\text{tail length, } l_t}$$

Curves of loss of $c_{l_{\max}}$ for tail lengths l_t of 2, 3, and 5 airfoil chord lengths are presented in figure 19 and can be used for determining the effective maximum section lift coefficient.

Effect of Various Modifications on Aerodynamic Section Characteristics

Effect of moving the two flaps as a unit.— In figures 20 and 21 are presented the aerodynamic section characteristics of the airfoil showing the effect of moving the rear flap and fore flap A as a unit. Figure 20 indicates that a 0.01c displacement of the flaps upward perpendicular to the airfoil chord had only a small adverse effect; however, a 0.01c movement of the flaps downward was quite critical because greatly decreased values of c_l and increased values of c_{d_0} were obtained.

The effect of a forward movement of 0.01c of the flaps is shown in figure 21; only a slight effect in the aerodynamic characteristics was obtained.

From these data, it is indicated that some positions and deflections of the flaps are quite critical; that is, a movement of as little as 0.01c may appreciably alter the characteristics obtained.

Effect of the airfoil lower lip.— The effect of deflecting or removing the lower lip of the airfoil from its normal position is indicated in figures 22 and 23 for different flap configurations. It is indicated in figures 22 and 23 that slightly more favorable section characteristics may be obtained by removing or deflecting the lip. The profile drag appears to be slightly less with the lip off than with the lip deflected. Such a result indicates that a smoother slot entry ahead of the flaps may be desirable. Although no data were obtained at small flap deflections, it is probable that the

smoother slot entry would be even more favorable under such conditions.

Effect of fore-flap size.— The effect of fore-flap size on the aerodynamic section characteristics is shown in figure 24. A comparison of the section characteristics of the airfoil for one configuration with fore flap B and two roughly comparable configurations with fore flap A indicates that the size of the fore flap has noticeable but small effects. The characteristics for the optimum position of fore flap B indicate values of c_l , c_{d_0} , and $c_{m(a.c.)_0}$ slightly greater than those of fore flap A at all angles of attack. With fore flap B, a value of $c_{l_{max}}$ of 3.35 was obtained, which is only 0.05 greater than the $c_{l_{max}}$ obtained with fore flap A. The configuration with the smaller fore flap that is more nearly geometrically similar to that of the larger fore flap (that is, with regard to airfoil fore-flap gap and fore-flap rear-flap gap) also gave higher values of the aerodynamic section characteristics at all angles of attack up to 6° than the optimum fore-flap-A configuration but gave lower values than the B configuration. The configuration with the smaller fore flap stalled, however, at a lower angle of attack and gave a value of $c_{l_{max}}$ of only 3.22.

CONCLUSIONS

Tests to determine the effect of flap position and deflection on the aerodynamic characteristics of an NACA 23012 airfoil with a double slotted flap having a chord 30 percent of the airfoil chord (0.30c) were conducted in the LMAL 7- by 10-foot tunnel. The results of these tests indicated that:

1. The use of a 0.30c double slotted flap on the NACA 23012 airfoil gave a maximum section lift coefficient of 3.30 which was larger than that of the 0.2566c and 0.40c single slotted flaps, equal to that of the 0.30c Fowler flap, but less than that of the 0.40c double slotted flap on the same airfoil.
2. The 0.30c double slotted flap gave profile-drag coefficients that were larger than those of the 0.2566c

and 0.40c single slotted flaps for section lift coefficients between 1.2 and 2.7 and were less than those of the single slotted flaps at values of section lift coefficients greater than 2.7; however, over the entire lift range, the present arrangement gave a higher profile drag than the 0.30c Fowler or 0.40c double slotted flaps.

3. The 0.30c double slotted flap gave negative section pitching-moment coefficients that were higher than those of the single and double slotted flaps but approximately equal to those of the Fowler flap at a given maximum section lift coefficient.

4. At high flap deflections and high section lift coefficients, a slight movement of the flaps from the optimum positions sometimes resulted in relatively large decreases in lift and increases in drag.

5. Removing or deflecting the airfoil lower lip improved the aerodynamic characteristics near maximum lift only slightly.

6. The use of a fore flap that was larger in both chord and thickness slightly increased the maximum section lift coefficient but also increased the section profile-drag and section pitching-moment coefficients.

Langley Memorial Aeronautical Laboratory,
National Advisory Committee for Aeronautics,
Langley Field, Va.

REFERENCES

1. Wenzinger, Carl J., and Harris, Thomas A.: Wind-Tunnel Investigation of an N.A.C.A. 23012 Airfoil with Various Arrangements of Slotted Flaps. Rep. No. 664, NACA, 1939.
2. Harris, Thomas A.: Wind-Tunnel Investigation of an N.A.C.A. 23012 Airfoil with Two Arrangements of a Wide-Chord Slotted Flap. T.W. No. 715, NACA, 1939.
3. Lowry, John G.: Wind-Tunnel Investigation of an NACA 23012 Airfoil with Several Arrangements of Slotted Flaps with Extended Lips. T.W. No. 808, NACA, 1941.
4. Harris, Thomas A., and Recant, Isadore G.: Wind-Tunnel Investigation of NACA 23012, 23021, and 23030 Airfoils Equipped with 40-Percent-Chord Double Slotted Flaps. Rep. No. 723, NACA, 1941.
5. Harris, Thomas A.: The 7 by 10 Foot Wind Tunnel of the National Advisory Committee for Aeronautics. Rep. No. 412, NACA, 1931.
6. Jacobs, Eastman N., and Sherman, Albert: Airfoil Section Characteristics as Affected by Variations of the Reynolds Number. Rep. No. 586, NACA, 1937.

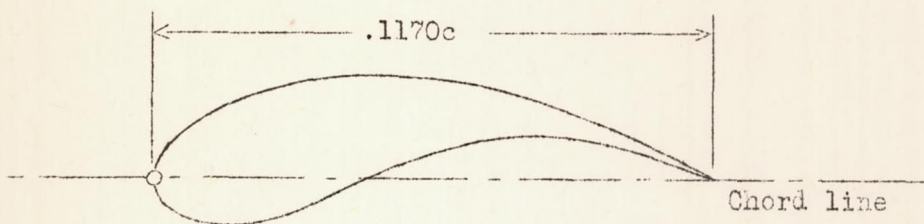
TABLE I

ORDINATES FOR AIRFOIL AND FLAPS

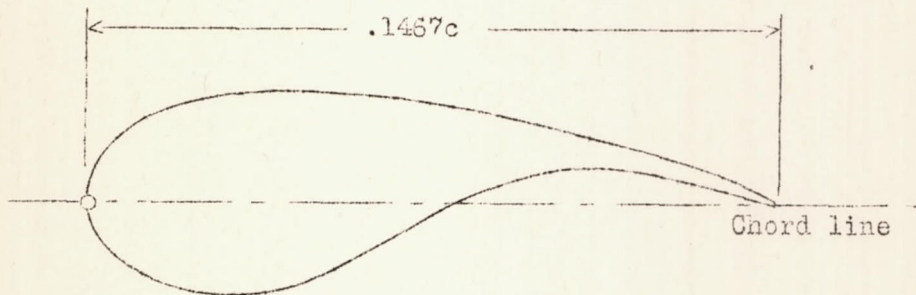
[Stations and ordinates in percent of airfoil chord]

| NACA 23012 airfoil | | | Rear flap | | | Fore flap A | | | Fore flap B | | |
|--|---------------|---------------|---|---------------|---------------|---|---------------|---------------|---|---------------|---------------|
| Station | Upper surface | Lower surface | Station | Upper surface | Lower surface | Station | Upper surface | Lower surface | Station | Upper surface | Lower surface |
| 0 | ---- | 0 | 0 | -1.29 | -1.29 | 0 | 0 | 0 | 0 | 0 | 0 |
| 1.25 | 2.67 | -1.23 | .40 | -.32 | -2.05 | .5 | .81 | -.71 | 1.39 | 1.72 | -1.75 |
| 2.5 | 3.61 | -1.71 | .72 | .04 | -2.21 | 1.0 | 1.20 | -.89 | 2.78 | 2.11 | -1.97 |
| 5 | 4.91 | -2.26 | 1.36 | .61 | -2.36 | 1.5 | 1.48 | -.98 | 4.17 | 2.28 | -1.78 |
| 7.5 | 5.80 | -2.61 | 2.00 | 1.04 | -2.41 | 2.0 | 1.69 | -.98 | 5.56 | 2.30 | -1.22 |
| 10 | 6.43 | -2.92 | 2.64 | 1.40 | -2.41 | 3.0 | 1.97 | -.74 | 6.94 | 2.14 | -.528 |
| 15 | 7.19 | -3.50 | 3.92 | 1.94 | ----- | 4.0 | 2.10 | -.36 | 8.33 | 1.92 | .222 |
| 20 | 7.50 | -3.97 | 5.20 | 2.30 | ----- | 5.0 | 2.12 | .08 | 9.72 | 1.61 | .667 |
| 25 | 7.60 | -4.28 | 5.66 | ----- | -2.16 | 6.0 | 2.04 | .44 | 11.11 | 1.25 | .722 |
| 30 | 7.55 | -4.46 | 6.48 | 2.53 | ----- | 7.0 | 1.88 | .69 | 12.50 | .806 | .50 |
| 40 | 7.14 | -4.48 | 7.76 | 2.63 | ----- | 8.0 | 1.61 | .84 | 13.89 | .306 | .167 |
| 50 | 6.41 | -4.17 | 9.03 | 2.58 | ----- | 9.0 | 1.25 | .80 | 14.67 | 0 | -.052 |
| 60 | 5.47 | -3.67 | 10.31 | 2.46 | ----- | 10.0 | .82 | .54 | L. E. radius: 1.58 Center of L. E. radius located on chord line | | |
| 70 | 4.36 | -3.00 | 15.66 | 1.68 | -1.23 | 11.0 | .34 | .16 | | | |
| 80 | 3.08 | -2.16 | 20.66 | .92 | -.70 | 11.67 | ----- | .09 | | | |
| 90 | 1.68 | -1.23 | 25.66 | .13 | -.13 | 11.70 | 0 | -.10 | | | |
| 95 | .92 | -.70 | | | | | | | | | |
| 100 | .13 | -.13 | | | | | | | | | |
| L. E. radius: 1.58 Slope of radius through end of chord: 0.305 | | | L. E. radius: 0.91 Center of L. E. arc: Upper surface, 0.91 Lower surface, -1.29 | | | L. E. radius: 0.75 Center of L. E. radius located on chord line | | | | | |

Ir-469



Fore flap A



Fore flap B

Figure 2.- Sections of the two fore flaps used in the investigation.

L-469

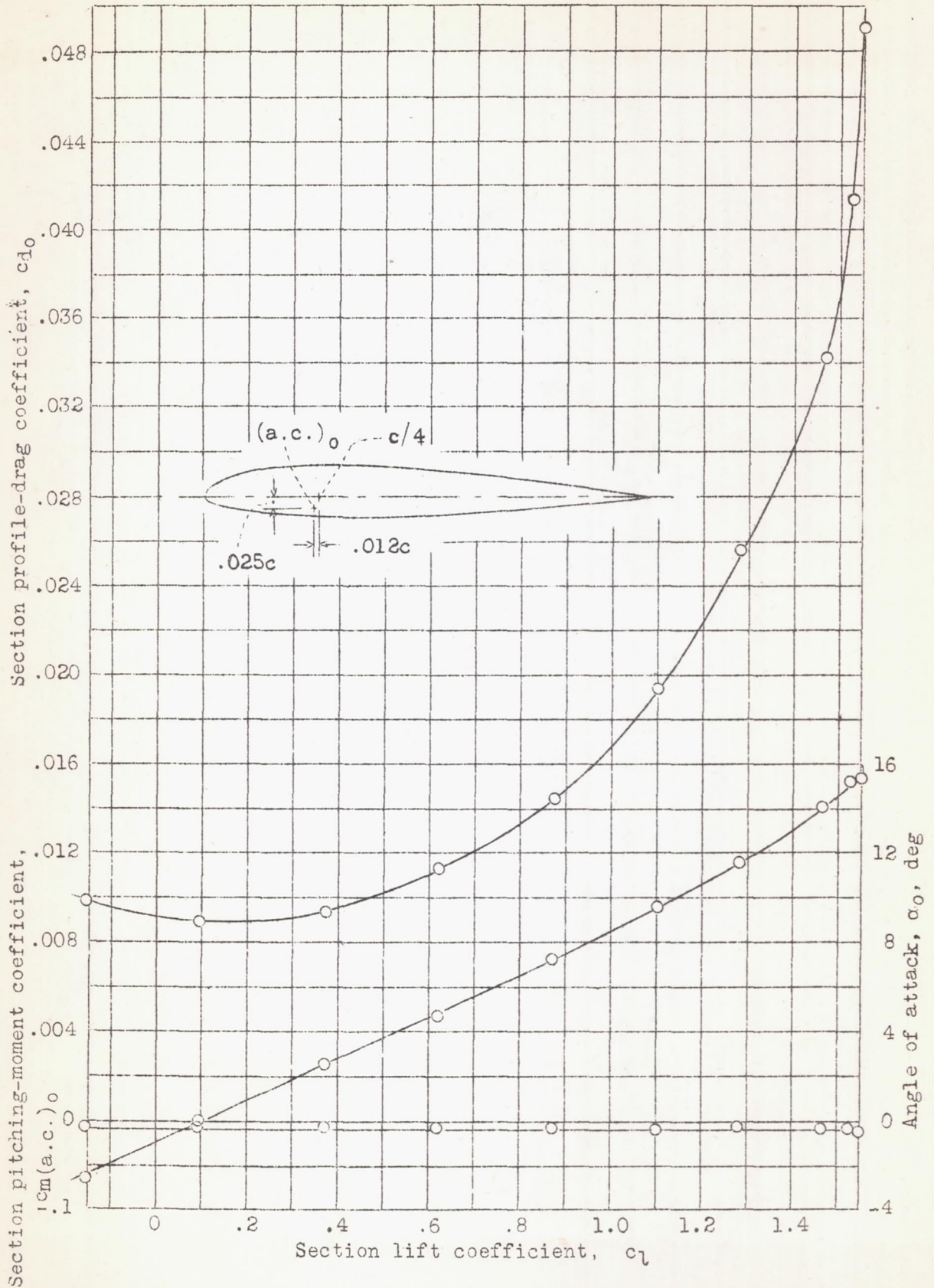
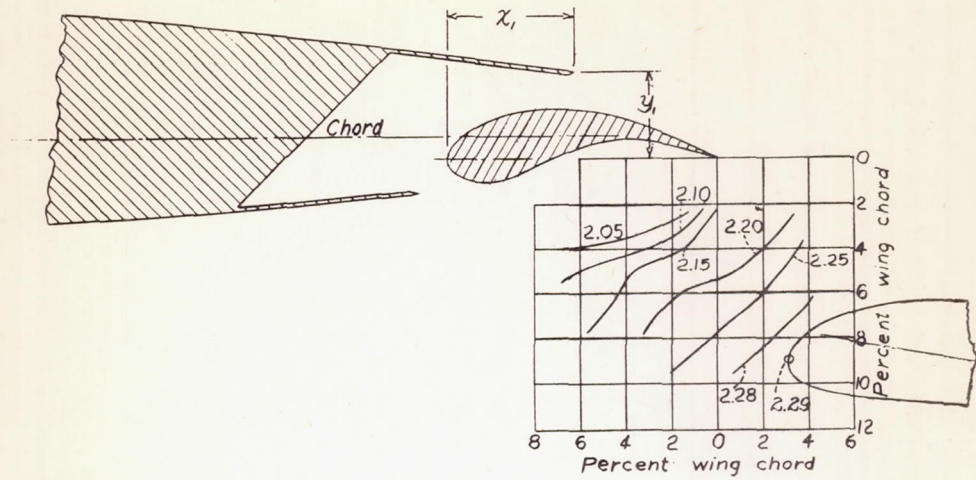
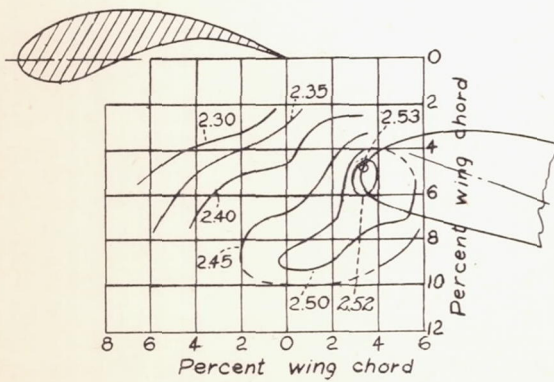


Figure 3.- Aerodynamic section characteristics of NACA 23012 plain airfoil. (From reference 1.)

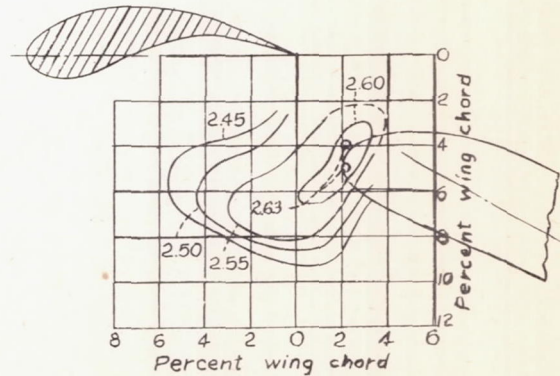
697-7



(a) $\delta_f = 10^\circ$.



(b) $\delta_f = 20^\circ$.



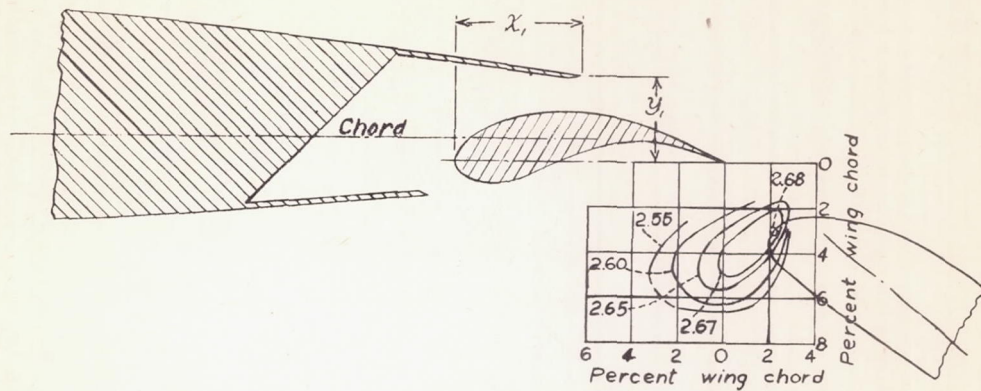
(c) $\delta_f = 30^\circ$.

Figure 4.- Contours of rear-flap position for $c_{l,max}$. Fore flap A, position 1; $\delta_{f1} = 0^\circ$; $x_1 = 5.59$; $y_1 = 3.72$. (Values of x_1, y_1 are given in percent airfoil chord.)

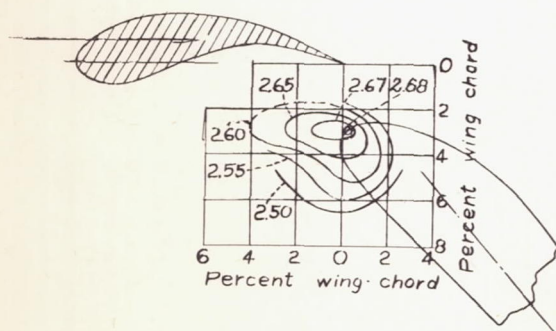
L-469

NACA

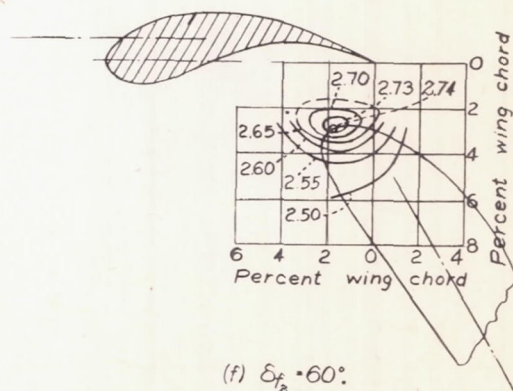
Figs. 4d,ef



(d) $\delta_{f_2} = 40^\circ$.



(e) $\delta_{f_2} = 50^\circ$.



(f) $\delta_{f_2} = 60^\circ$.

Figure 4. - Concluded.

694-7

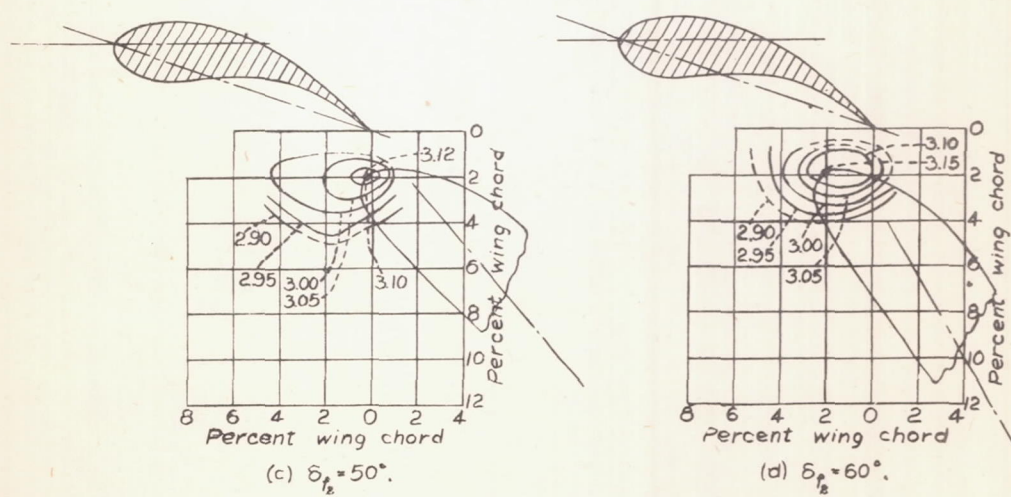
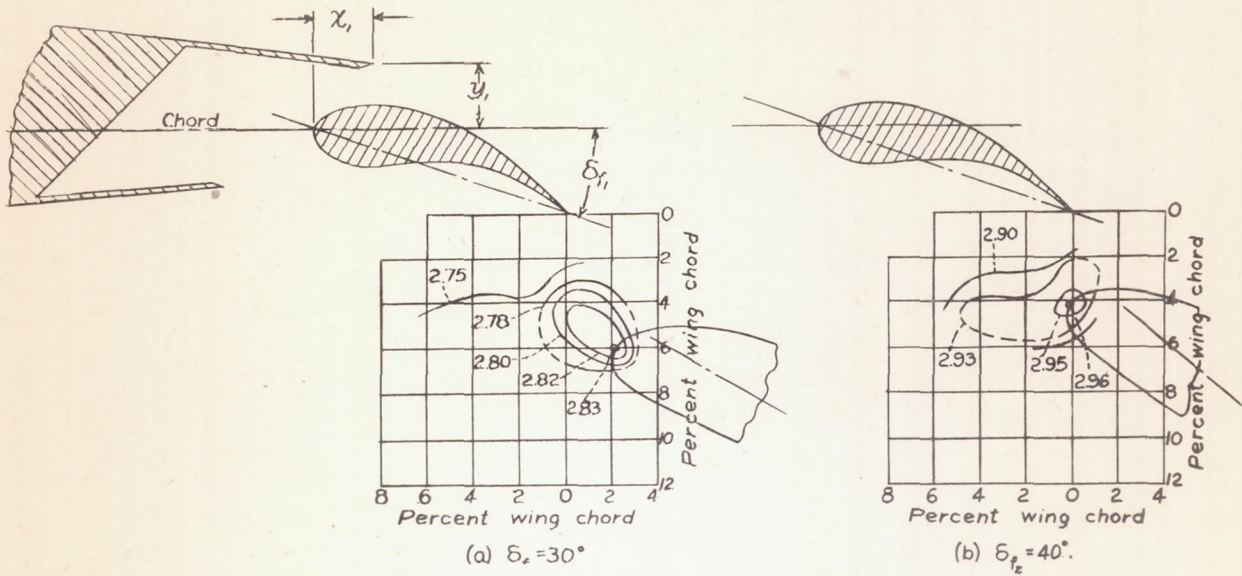
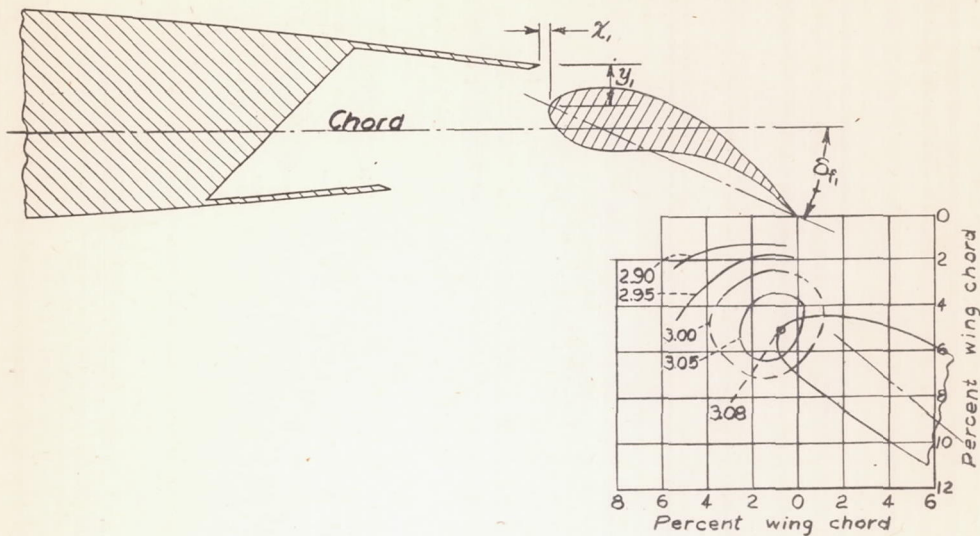
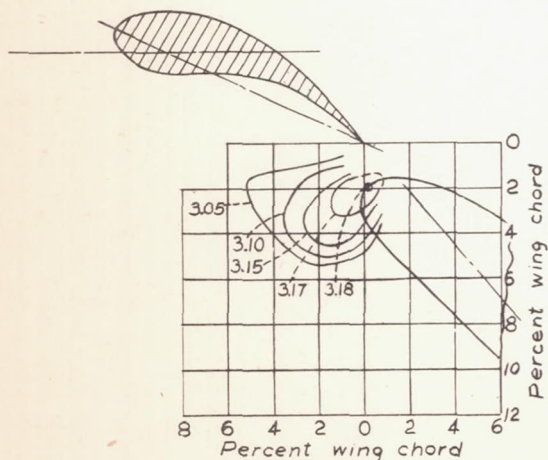


Figure 5- Contours of rear-flap position for C_{Lmax} . Fore flap A, position 2; $\delta_{f1} = 20^\circ$; $x_1 = 2.59$; $y_1 = 2.72$. (Values of x_1, y_1 are given in percent airfoil chord.)

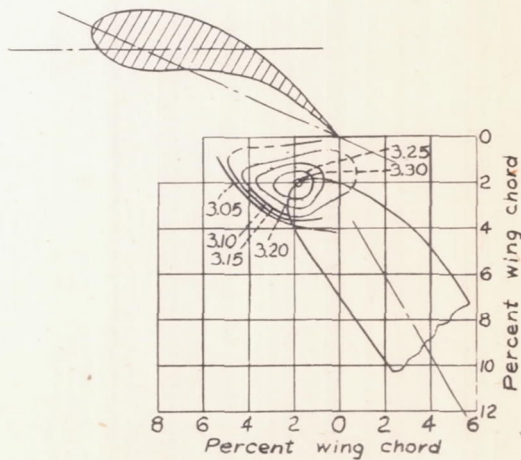
L-469



(a) $\delta_{f_2} = 40^\circ$.



(b) $\delta_{f_2} = 50^\circ$.



(c) $\delta_{f_2} = 60^\circ$.

Figure 6.- Contours of rear-flap position for $C_{2,max}$. Fore flap A, position 3; $\delta_{f_1} = 25^\circ$; $x_1 = -0.41$, $y_1 = 1.72$. (Values of x_1 , y_1 are given in percent airfoil chord)

L-469

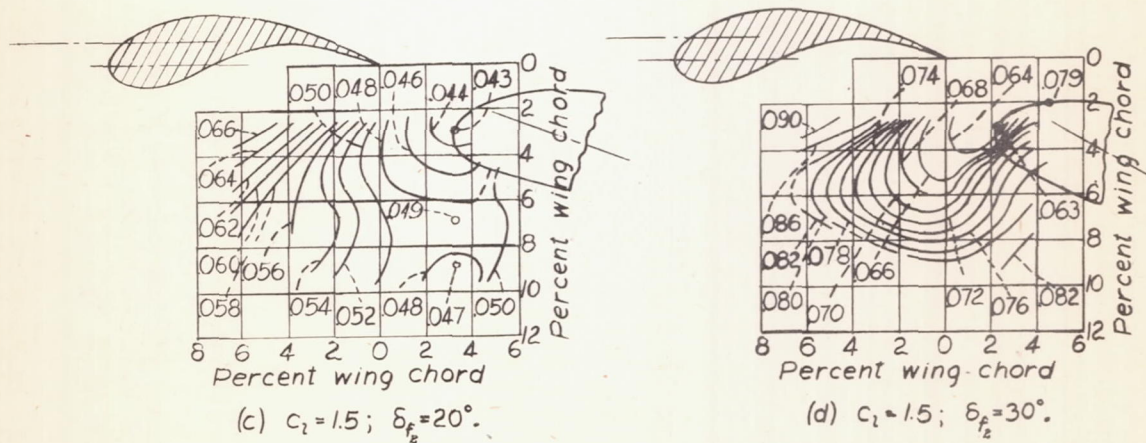
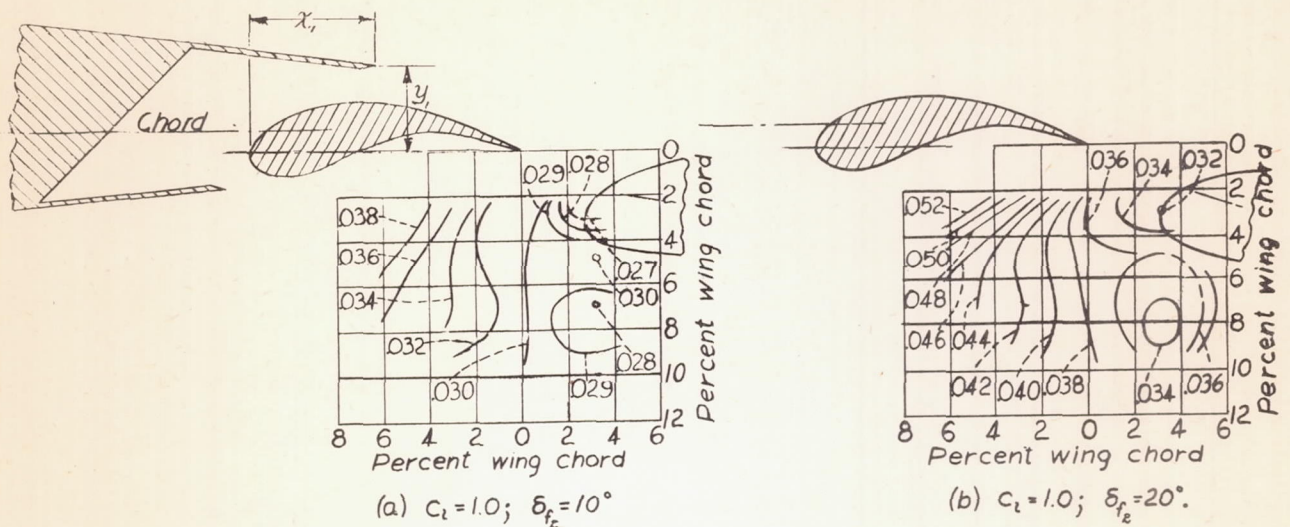


Figure 7.- Contours of rear-flap position for c_d . Fore flap A, position 1; $\delta_{f_1} = 0^\circ$; $x_f = 5.59$; $y_f = 3.72$. (Values of x_f , y_f are given in percent airfoil chord.)

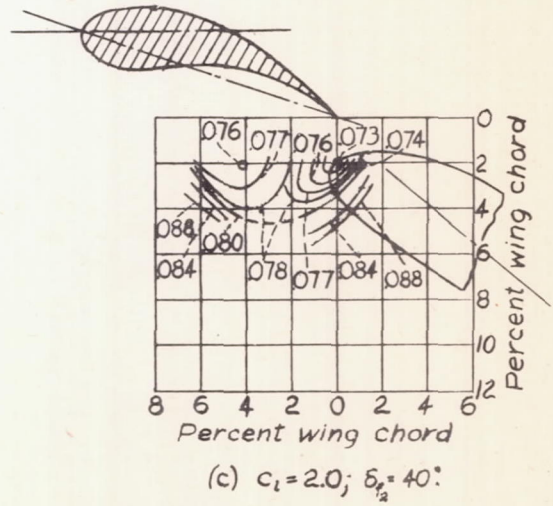
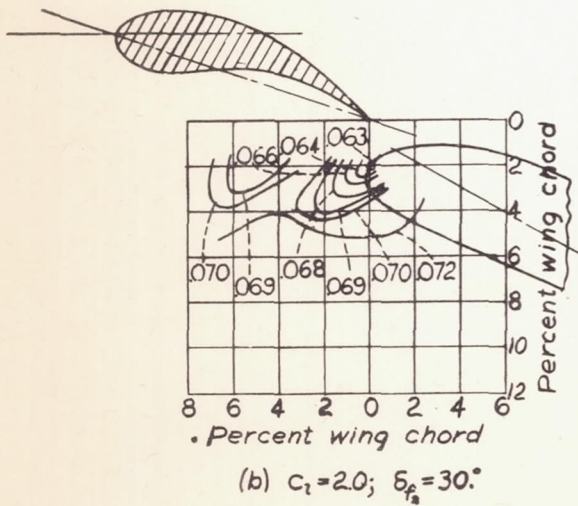
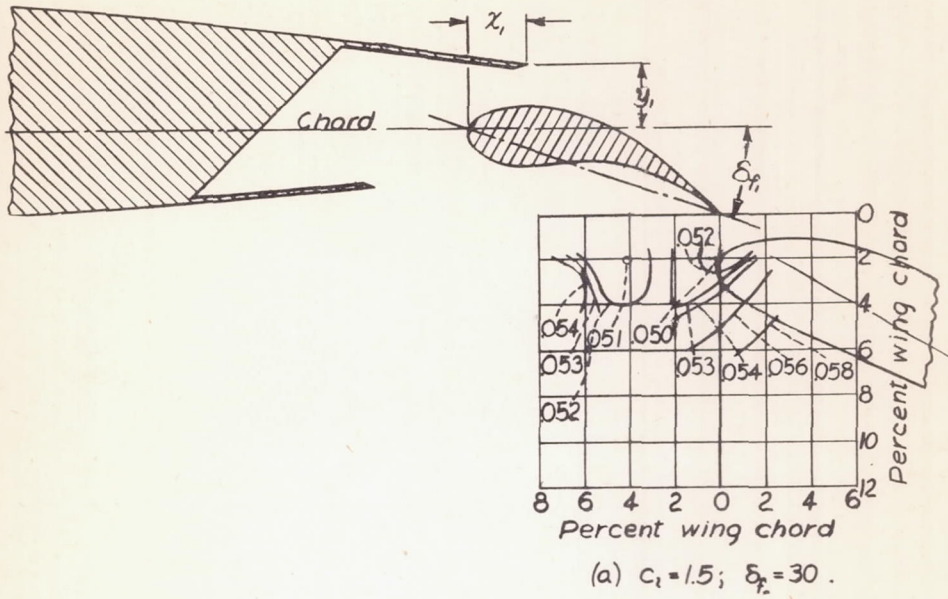
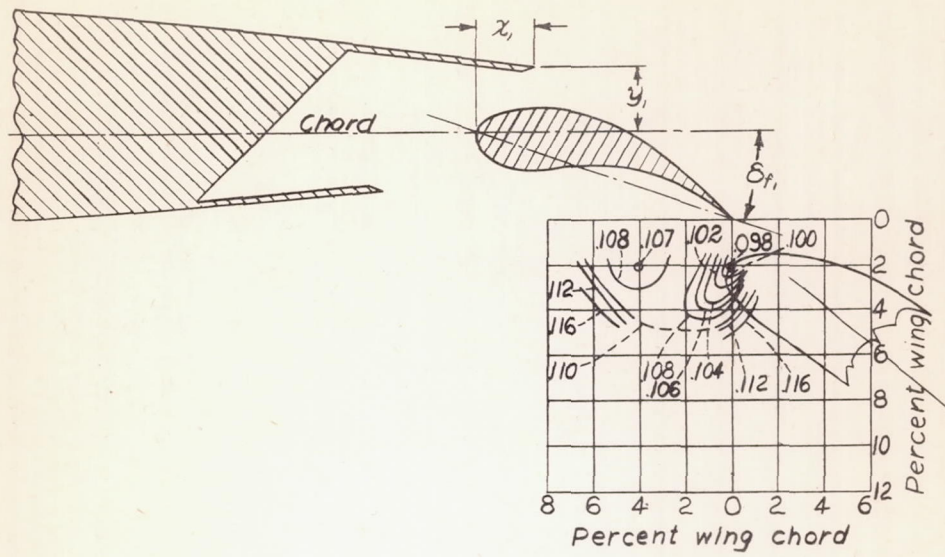
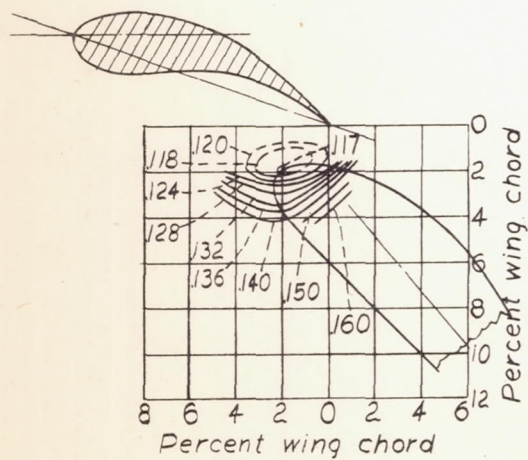


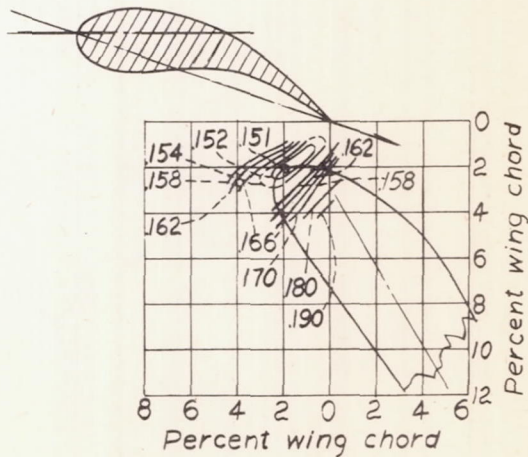
Figure 8.-Contours of rear-flap position for c_d . Fore flap A, position 2; $\delta_f = 20^\circ$; $x_f = 2.59$; $y_f = 2.72$. (Values of x_f, y_f are given in percent airfoil chord.)



(d) $C_l = 2.5$; $\delta_f = 40^\circ$



(e) $C_l = 2.5$; $\delta_f = 50^\circ$



(f) $C_l = 2.5$; $\delta_f = 60^\circ$

Figure 8.- Concluded.

L-469

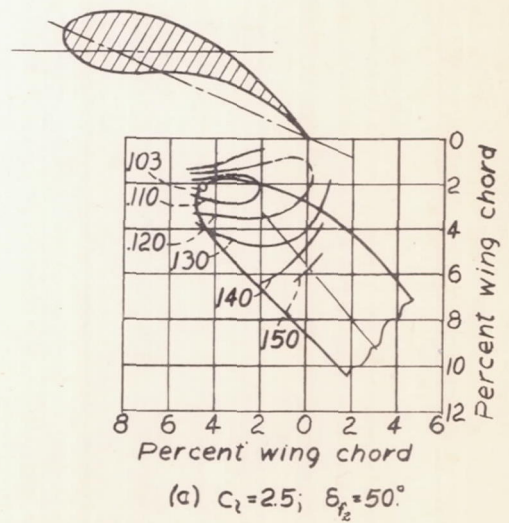
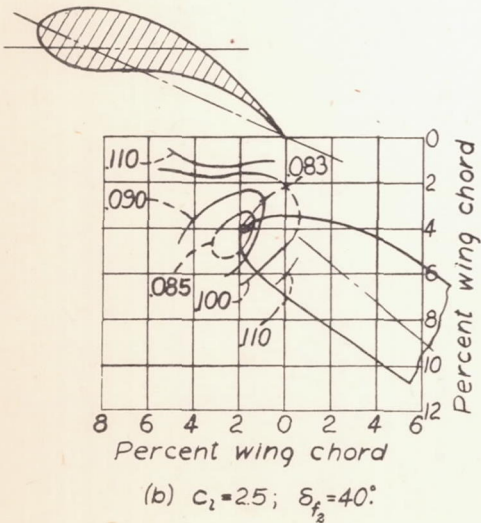
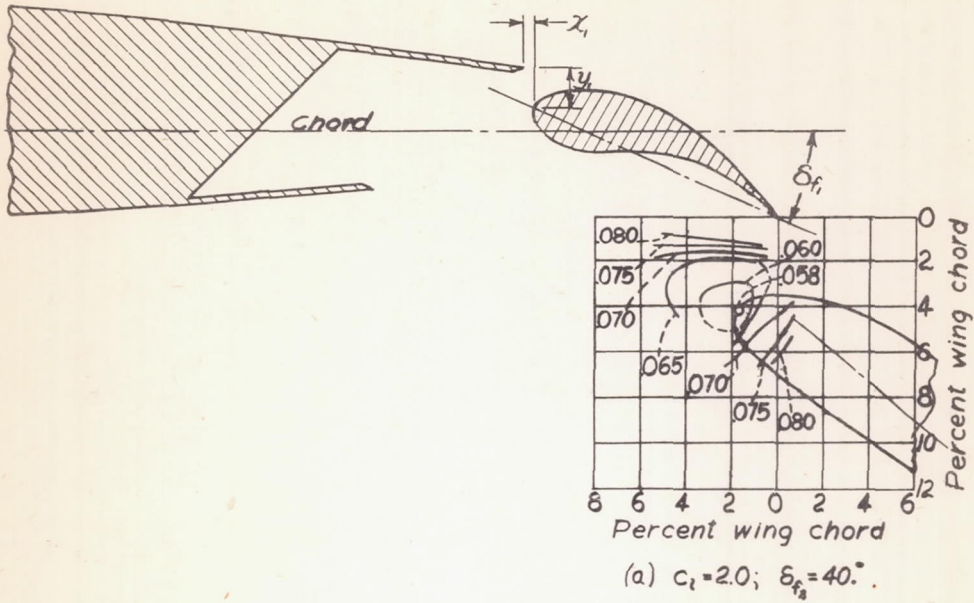
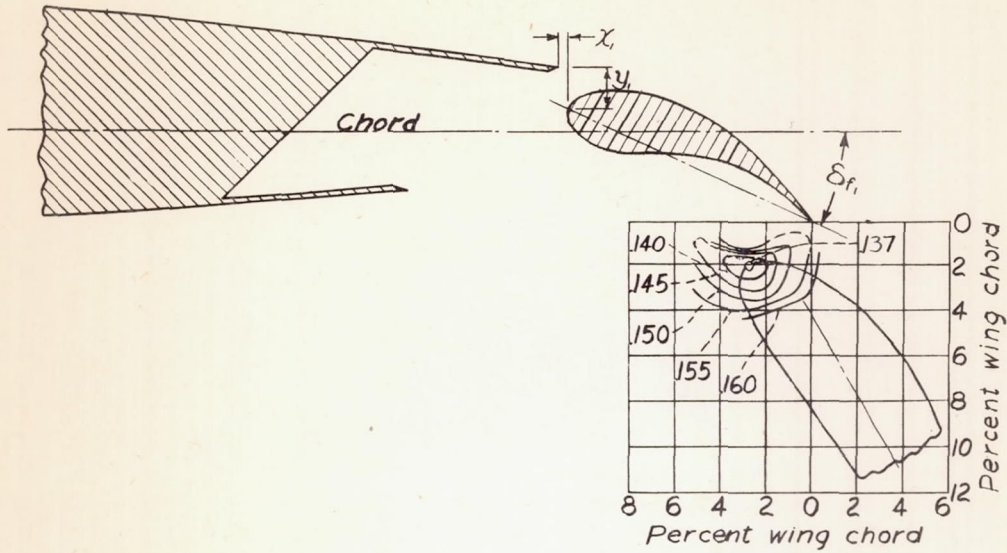
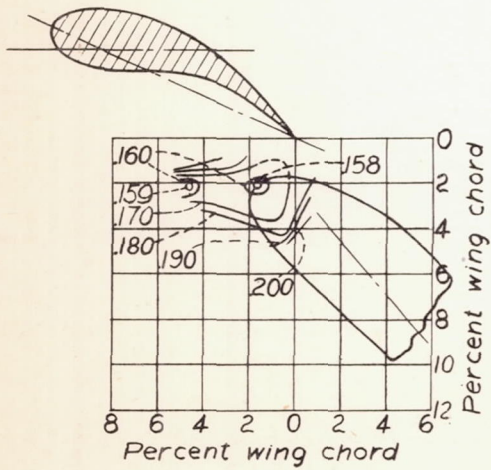


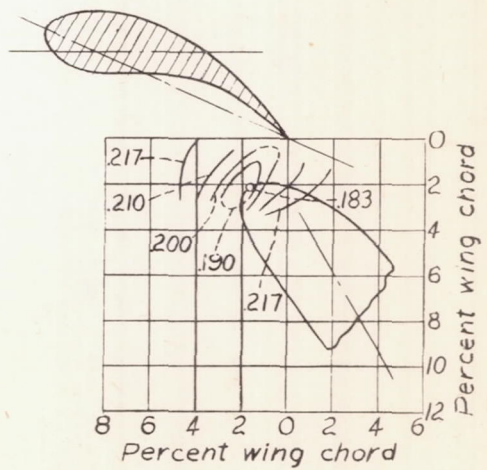
Figure 9. - Contours of rear-flap position for c_{d_0} . Fore flap A, position 3; $\delta_{f_1} = 25^\circ$; $x_1 = -0.41$; $y_1 = 1.72$. (Values of x_1, y_1 are given in percent airfoil chord.)



(d) $c_l = 2.5$; $\delta_{f_2} = 60^\circ$.



(e) $c_l = 3.0$; $\delta_{f_2} = 50^\circ$.



(f) $c_l = 3.0$; $\delta_{f_2} = 60^\circ$.

Figure 9. - Concluded.

L-469

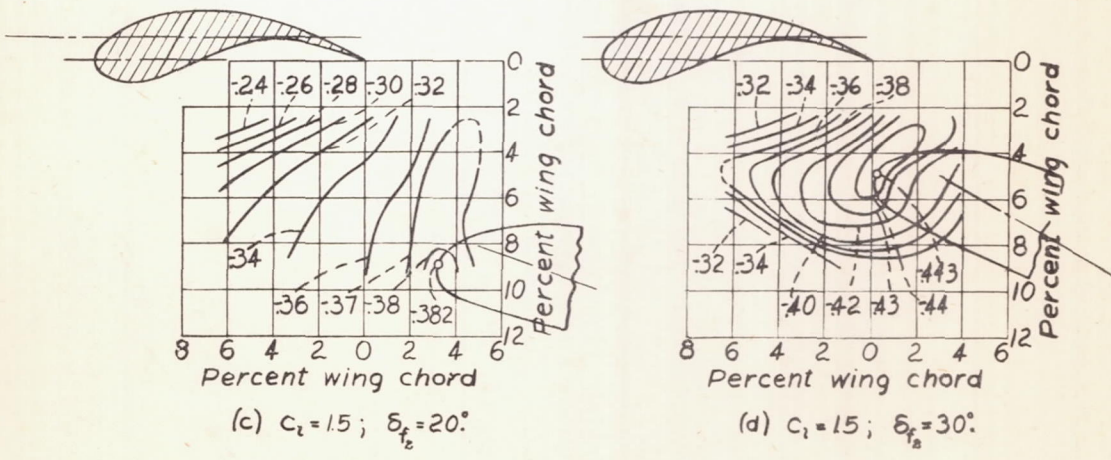
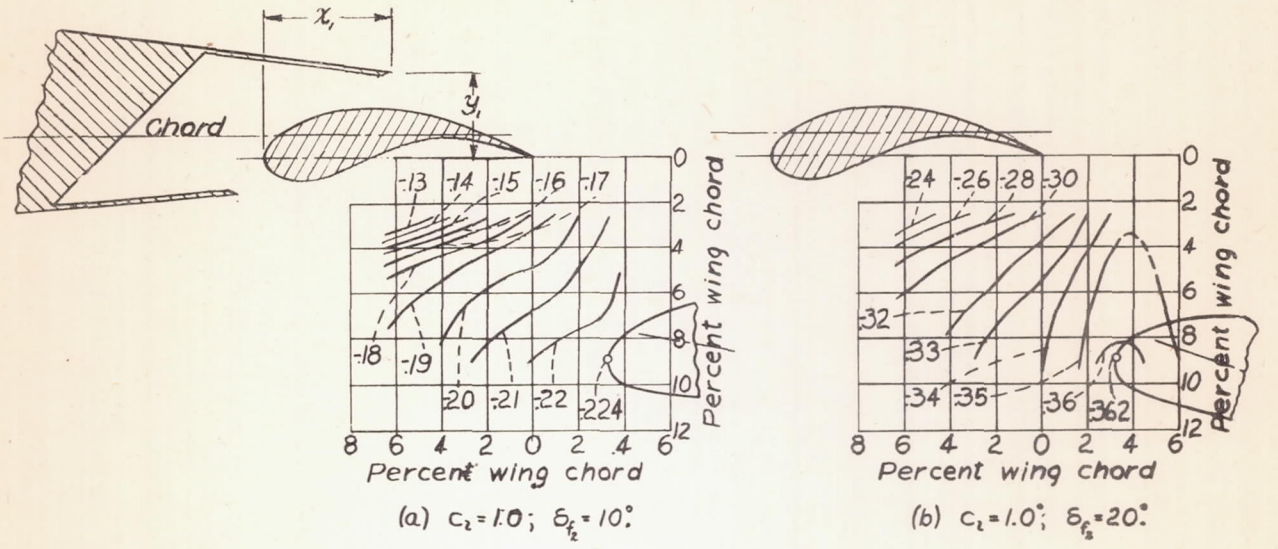


Figure 10.-Contours of rear-flap position for $C_{m(a.c.)}$. Fore flap A, position 1; $\delta_f = 0^\circ$; $x_f = 5.59$; $y_f = 3.72$. (Values of x_f, y_f are given in percent airfoil chord.)

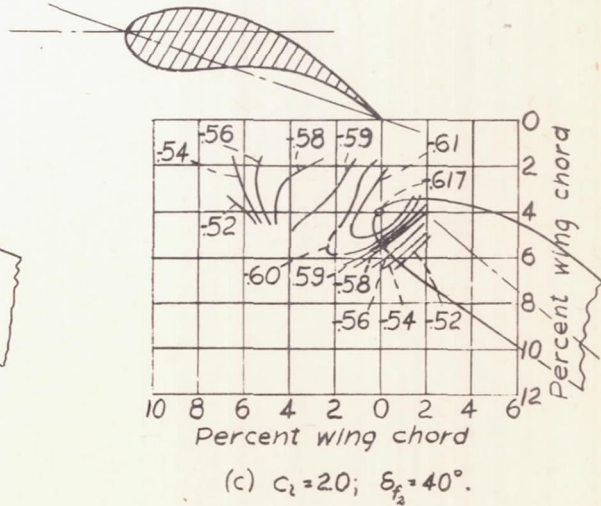
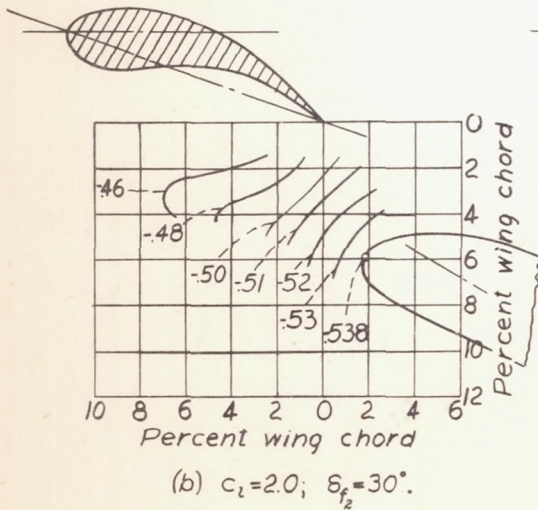
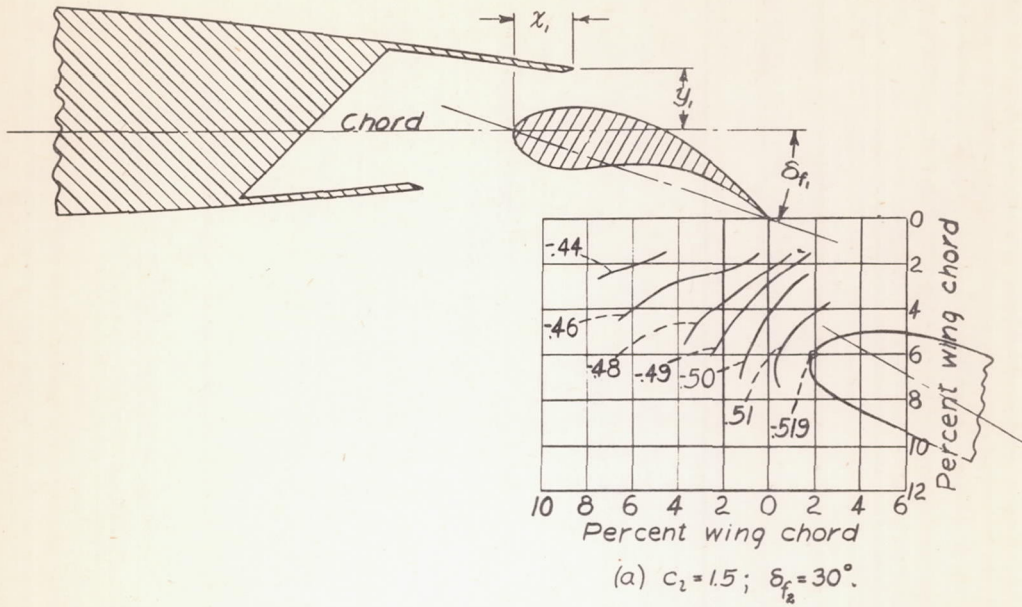
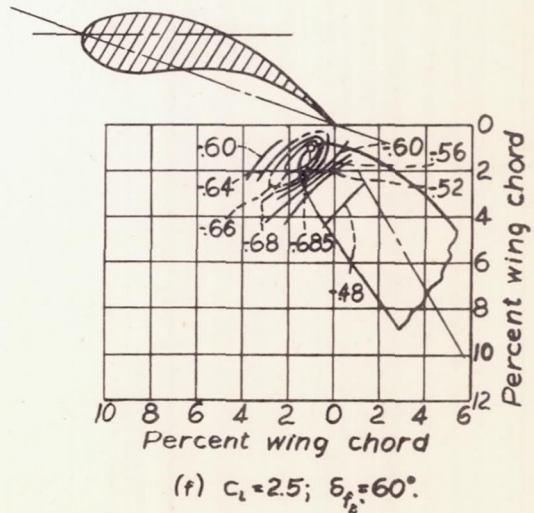
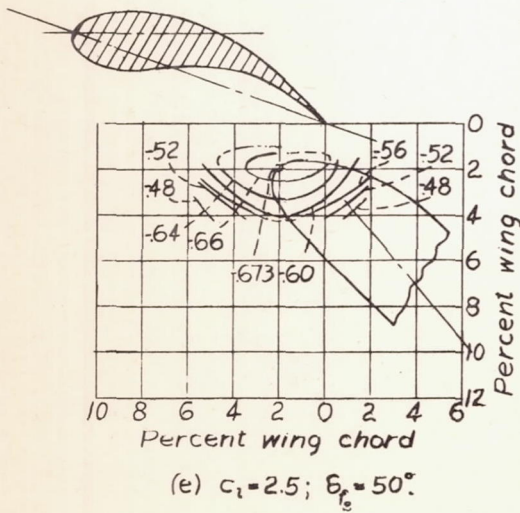
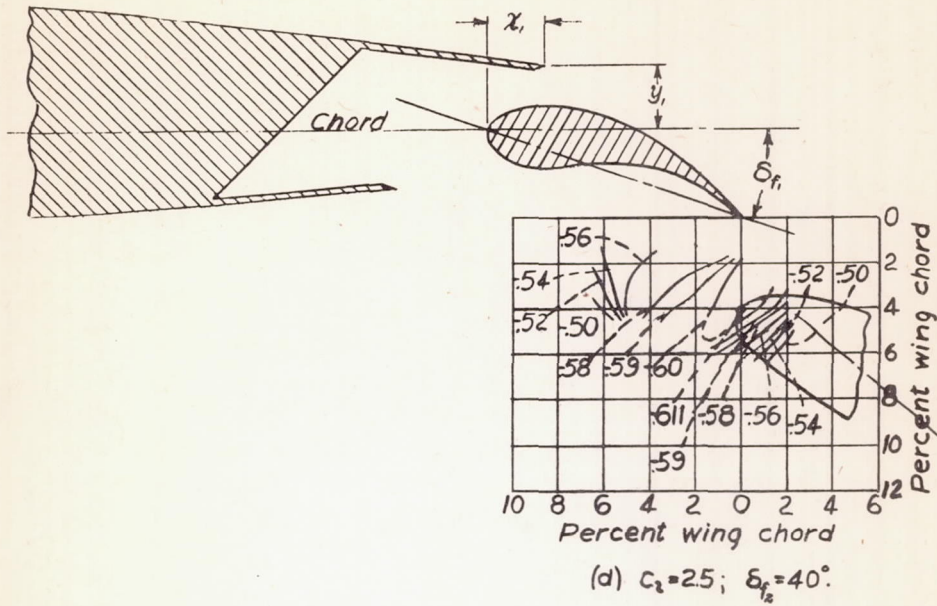


Figure 11.-Contours of rear-flap position for $c_{m(a.c.)}$. Fore flap A, position 2; $\delta_{f_1} = 20^\circ$; $x_1 = 2.59$; $y_1 = 2.72$. (Values of x_1, y_1 are given in percent airfoil chord.)

L-469

894-7



Figur 11. - Concluded

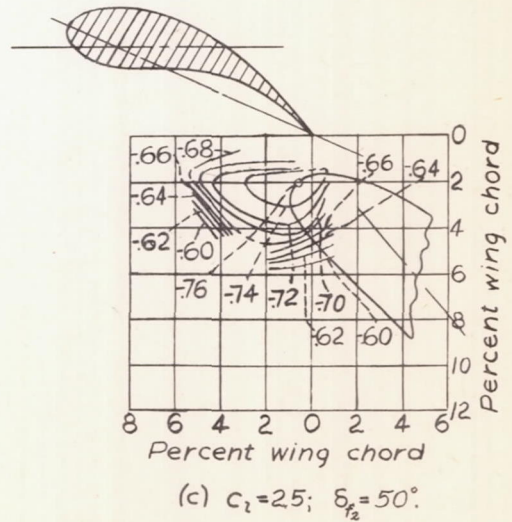
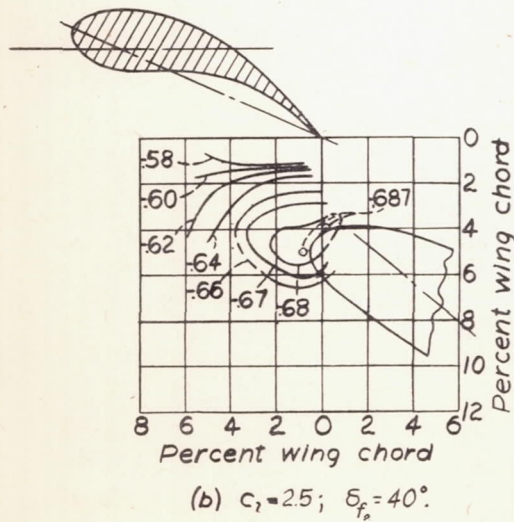
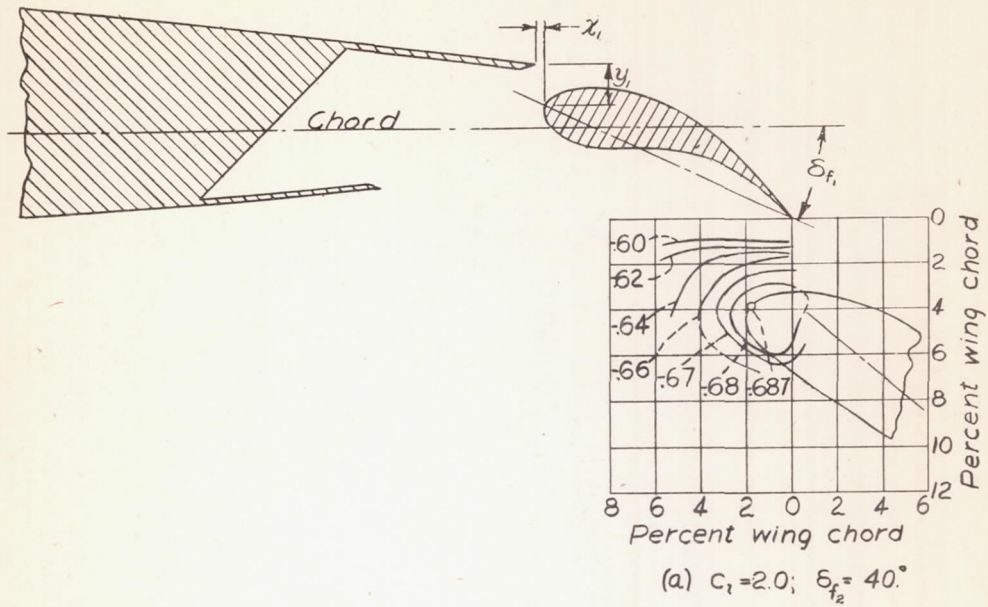


Figure 12.- Contours of rear-flap position for $C_{m(a.c.)_0}$. Fore flap A, position 3; $\delta_{f_1} = 25^\circ$; $x_1 = -0.41$; $y_1 = 1.72$. (Values of x_1, y_1 are given in percent airfoil chord.)

2-469

NACA

Figs. 12d, e, f

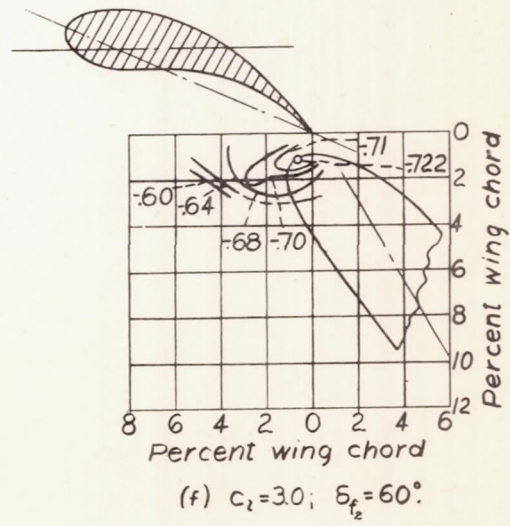
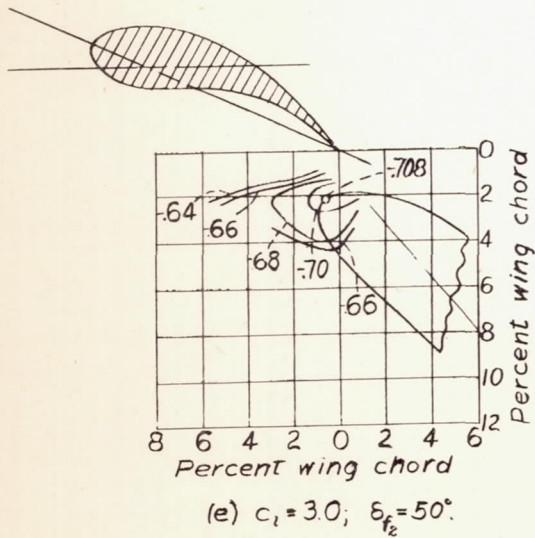
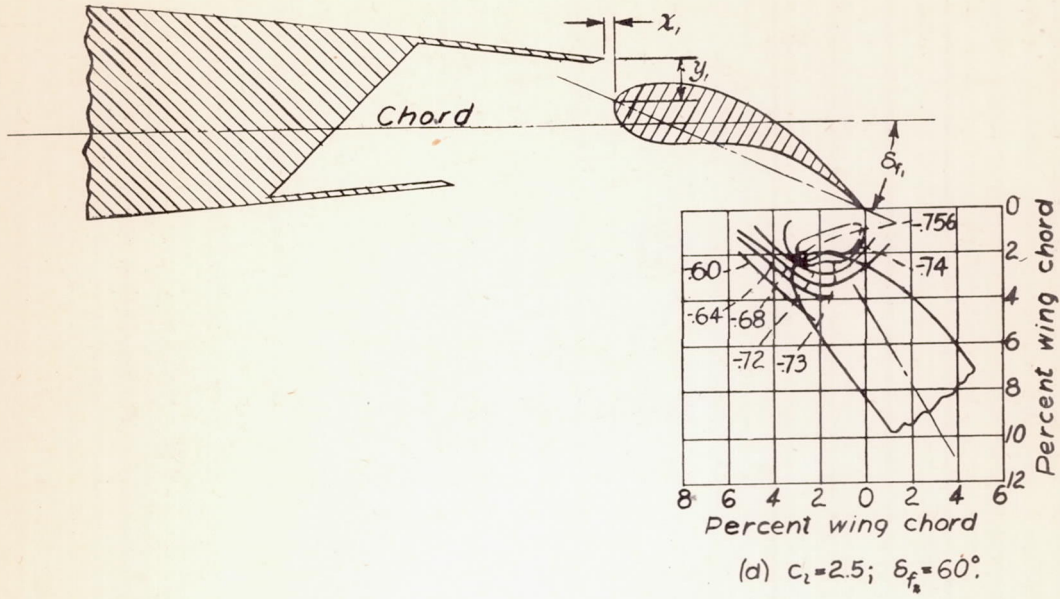
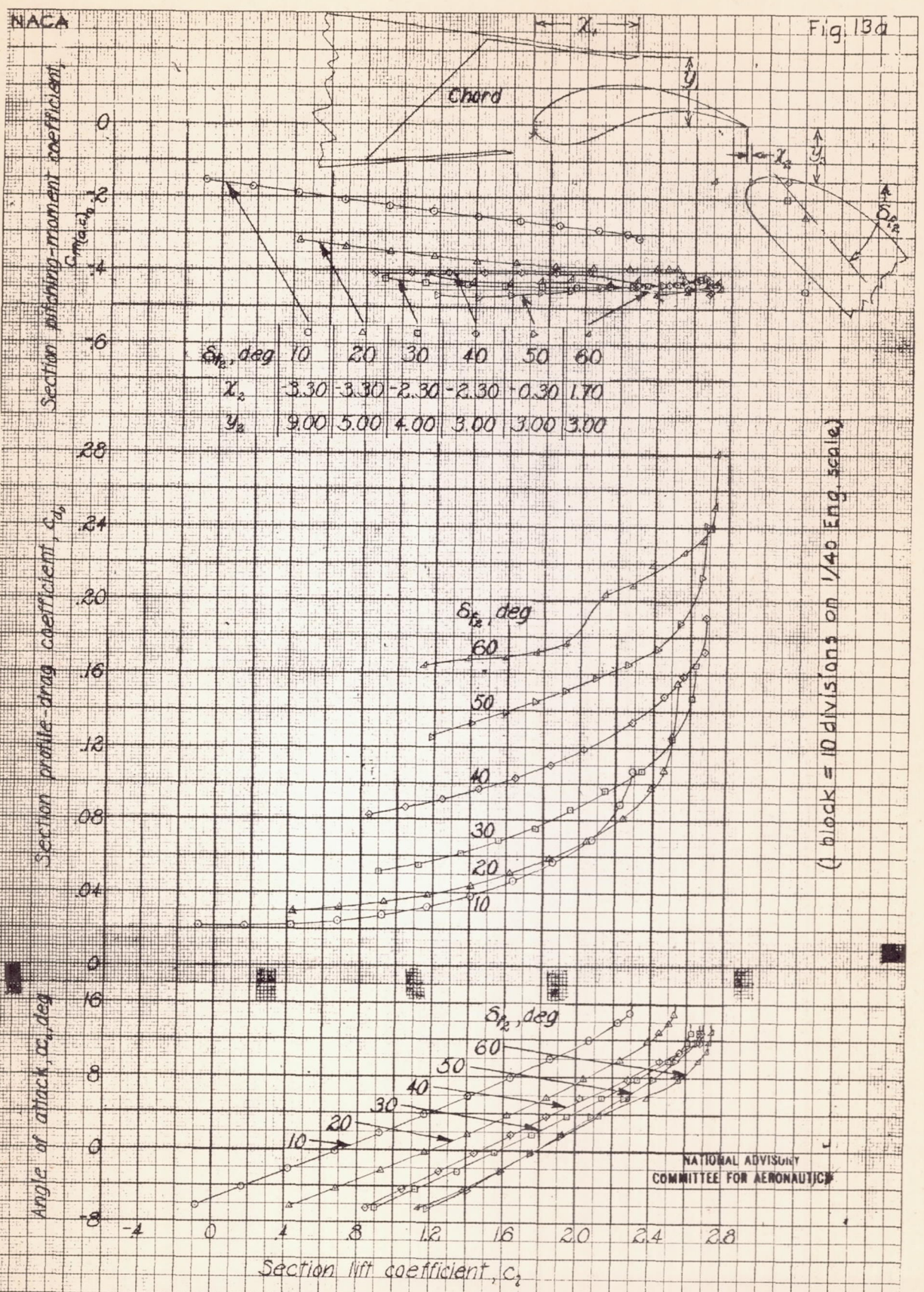


Figure 12. - Concluded.

L-469



(a) Rear-flap positions for $C_{l,max}$

Figure 13.-Aerodynamic section characteristics of NACA 23012 airfoil with a 0.30 c double slotted flap. Fore flap A, position 1; $\delta_{fl} = 0^\circ$; $x_1 = 5.59$, $y_1 = 3.72$. (Values of x_1 , y_1 , and x_2 , y_2 are given in percent airfoil chord.)

NATIONAL ADVISORY COMMITTEE FOR AERONAUTICS

Section pitching-moment coefficient, $C_{m, sec}$

0
-2
-4
-6

| δ_{F_2} , deg | 10 | 20 | 30 | 40 | 50 | 60 |
|----------------------|------|------|------|------|------|------|
| γ_{10} | 3.30 | 2.30 | 2.30 | 0.30 | 0.30 | 3.70 |
| U_2 | 3.00 | 3.00 | 3.00 | 3.00 | 3.00 | 3.00 |

Section profile-drag coefficient, $C_{D, sec}$

28
24
20
16
12
08
04
0

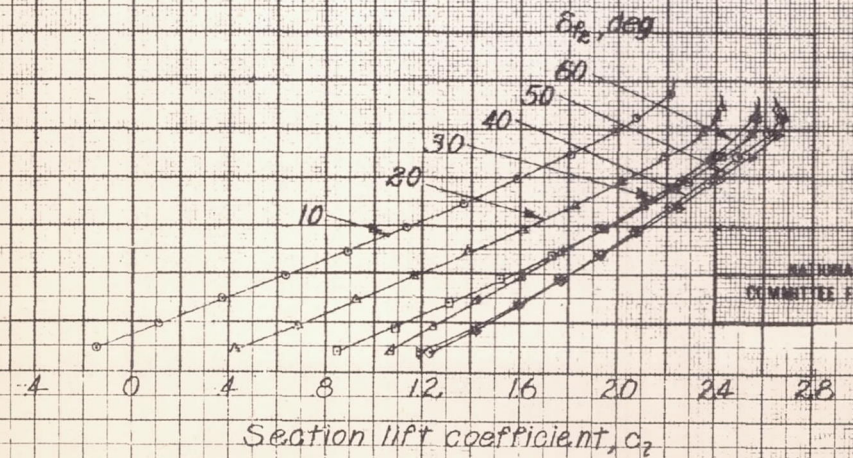
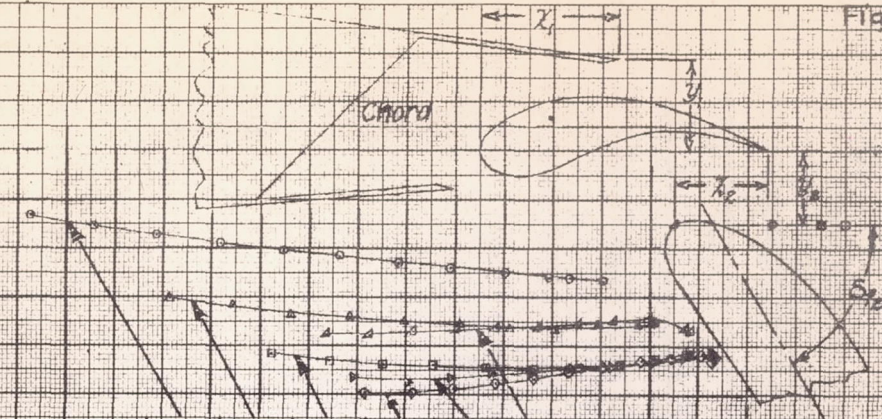
Angle of attack, α , deg

16
8
0
-8

Section lift coefficient, C_L

(b) Rear-flap positions for $C_{D, min}$

Figure 13- Concluded

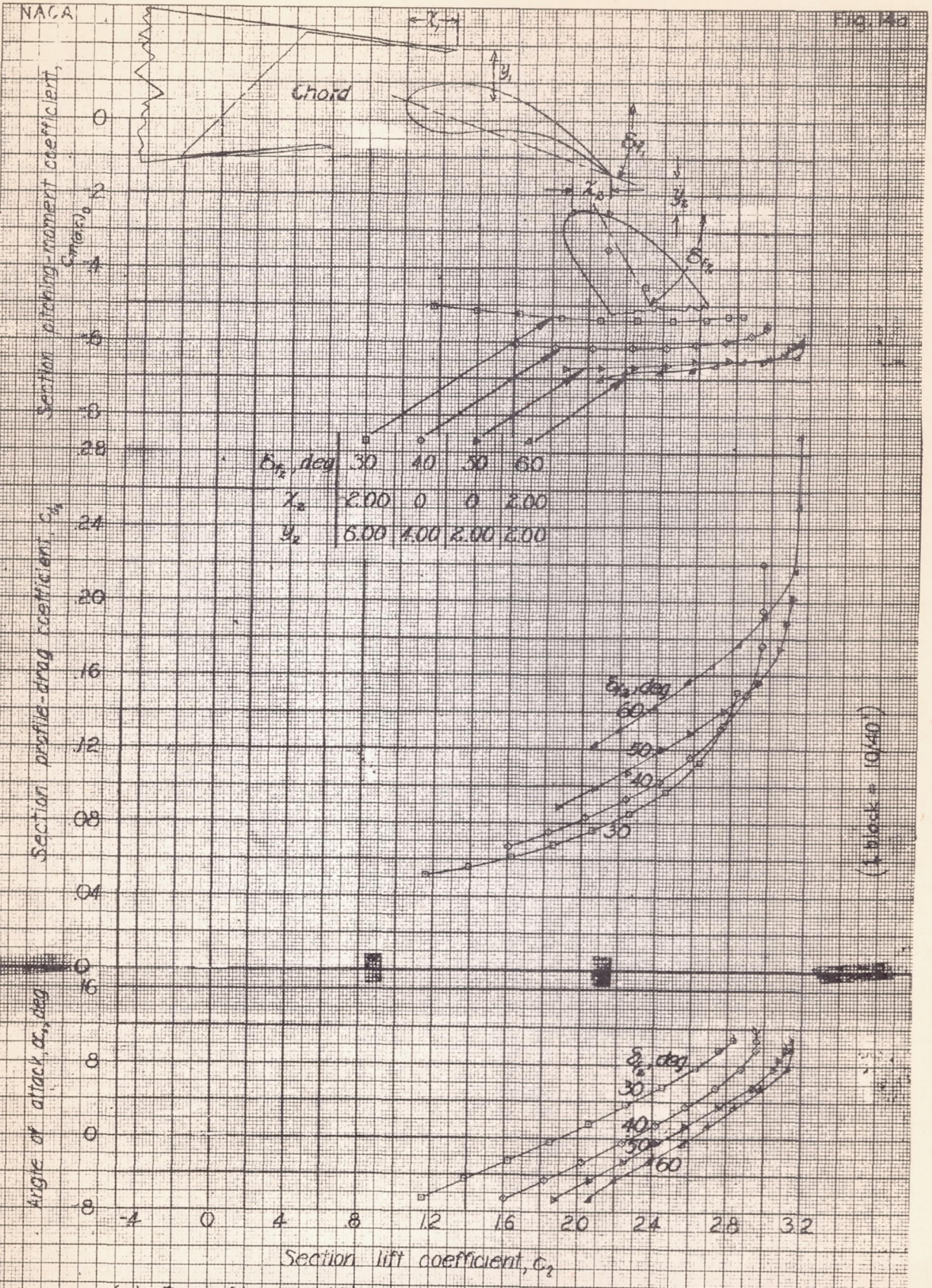


(1 block = 0/40)

NATIONAL ADVISORY
COMMITTEE FOR AERONAUTICS

L-469

L-469



(d) Rear flap positions for C_L max.

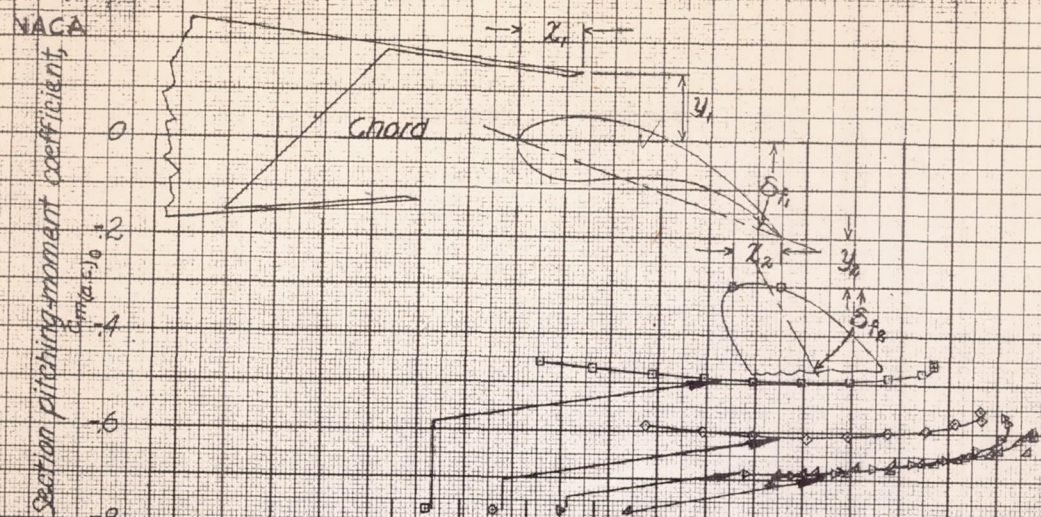
Figure 14 - Aerodynamic section characteristics of NACA 23012 airfoil with a 0.30c double-slotted flap. Fore flap A, position B; $\delta_{fl} = 20^\circ$; $x_1 = 2.59$, $y_1 = 2.72$. (Values of x_1 , y_1 , and x_2 , y_2 are given in percent airfoil chord)

Fig. 14a

(1 block = 10/40)

22-469

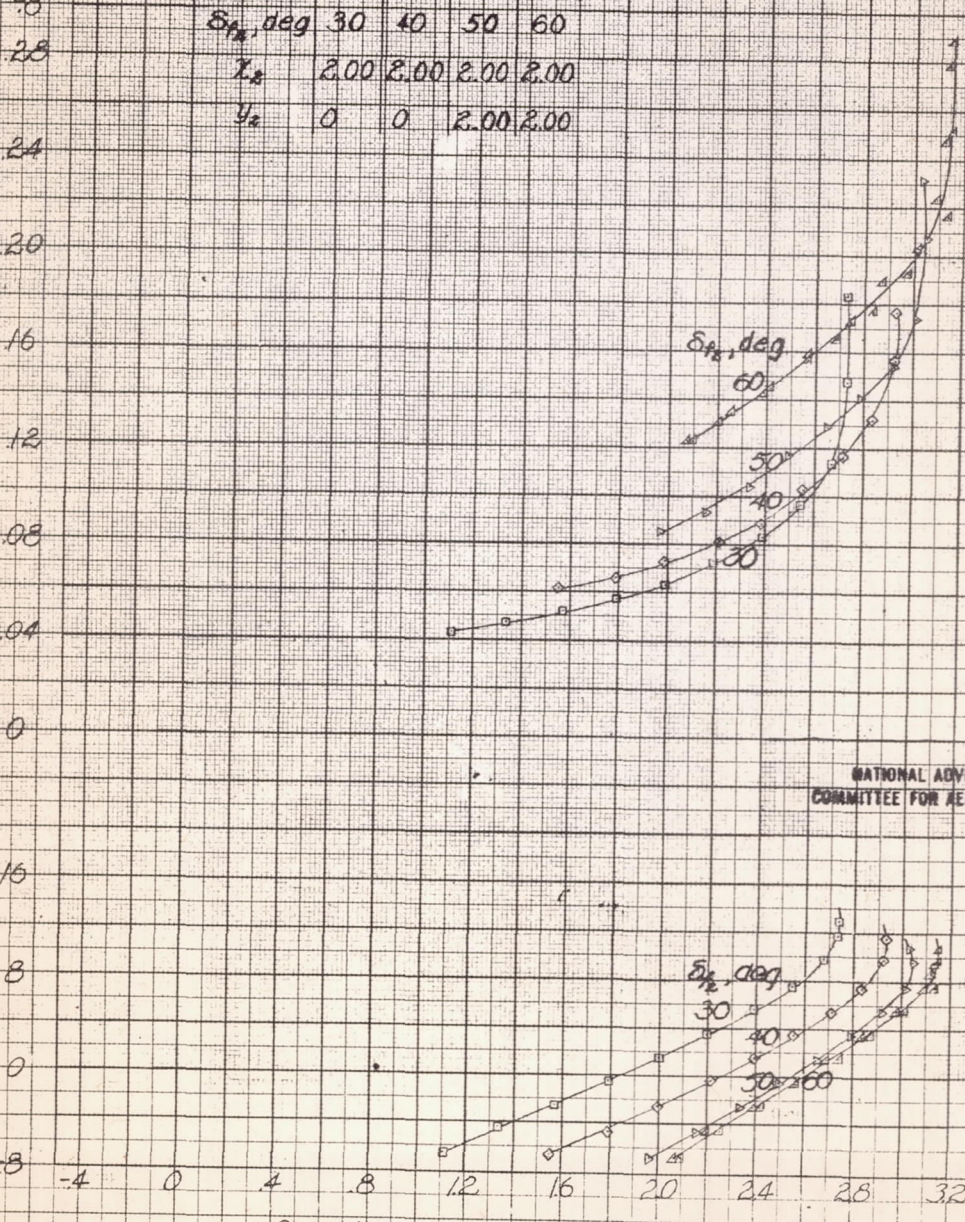
Fig. 14b



VACA
Section pitching-moment coefficient,
 $\frac{d_m}{c \rho V^2}$

Section profile-drag coefficient, C_{dp}

Angle of attack, α , deg



| δ_{fl} , deg | 30 | 40 | 50 | 60 |
|---------------------|------|------|------|------|
| x_{fl} | 2.00 | 2.00 | 2.00 | 2.00 |
| y_{fl} | 0 | 0 | 2.00 | 2.00 |

δ_{fl} , deg
60
50
40
30

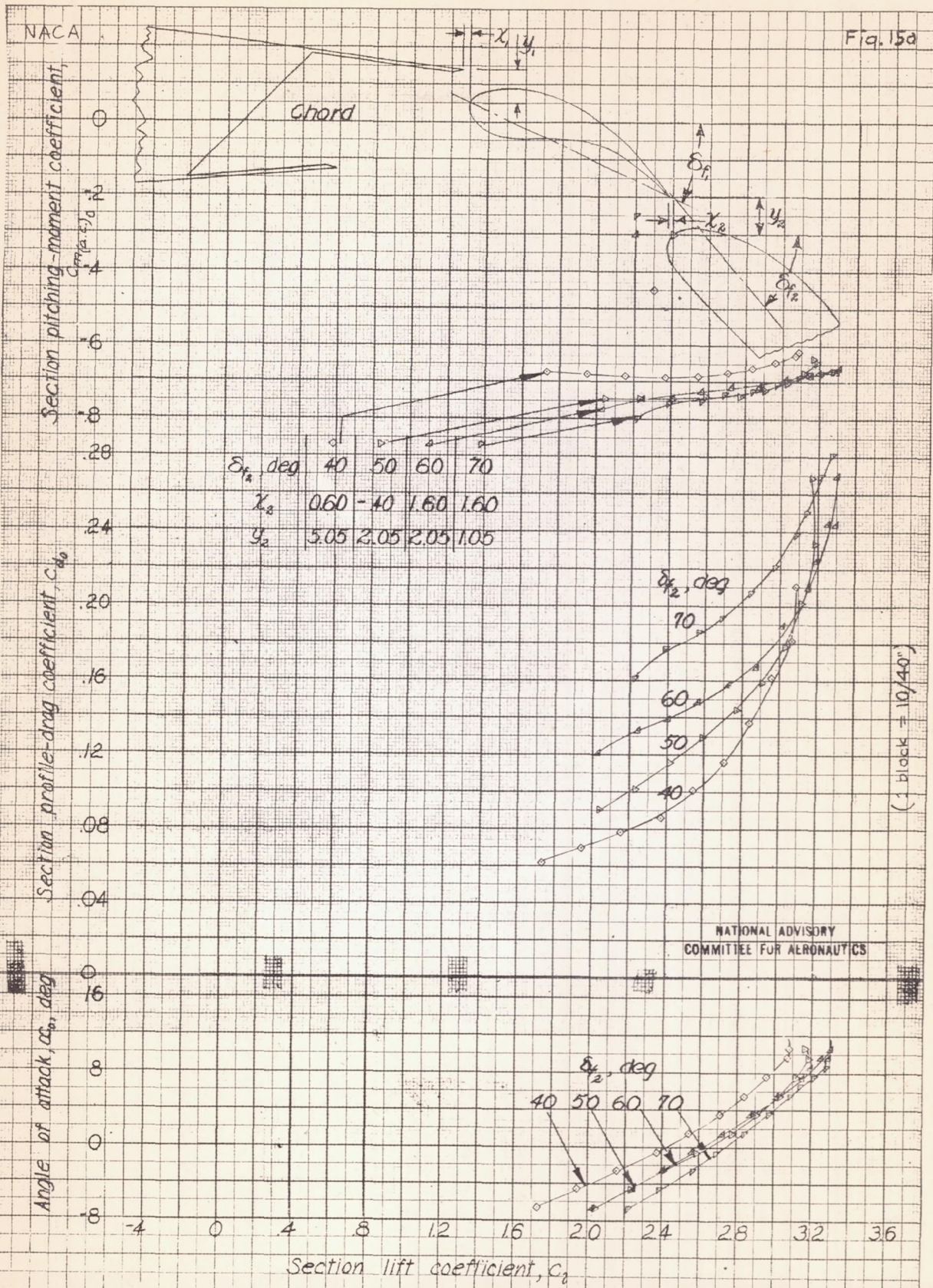
(1 block = 10/40)

NATIONAL ADVISORY
COMMITTEE FOR AERONAUTICS

Section lift coefficient, c_l

(b) Rear-flap positions for $C_{d_{min}}$ (Figure 14.- Concluded)

L-469



(a) Rear-flap positions for $C_{l, \max}$.

Figure 15.- Aerodynamic section characteristics of the NACA 23012 airfoil with a 0.30c double slotted flap. Fore flap A, position 3; $\delta_f = 25^\circ$; $x_1 = 0.41$; $y_1 = 1.72$. (Values of x_1, y_1 , and x_2, y_2 are given in percent airfoil chord.)

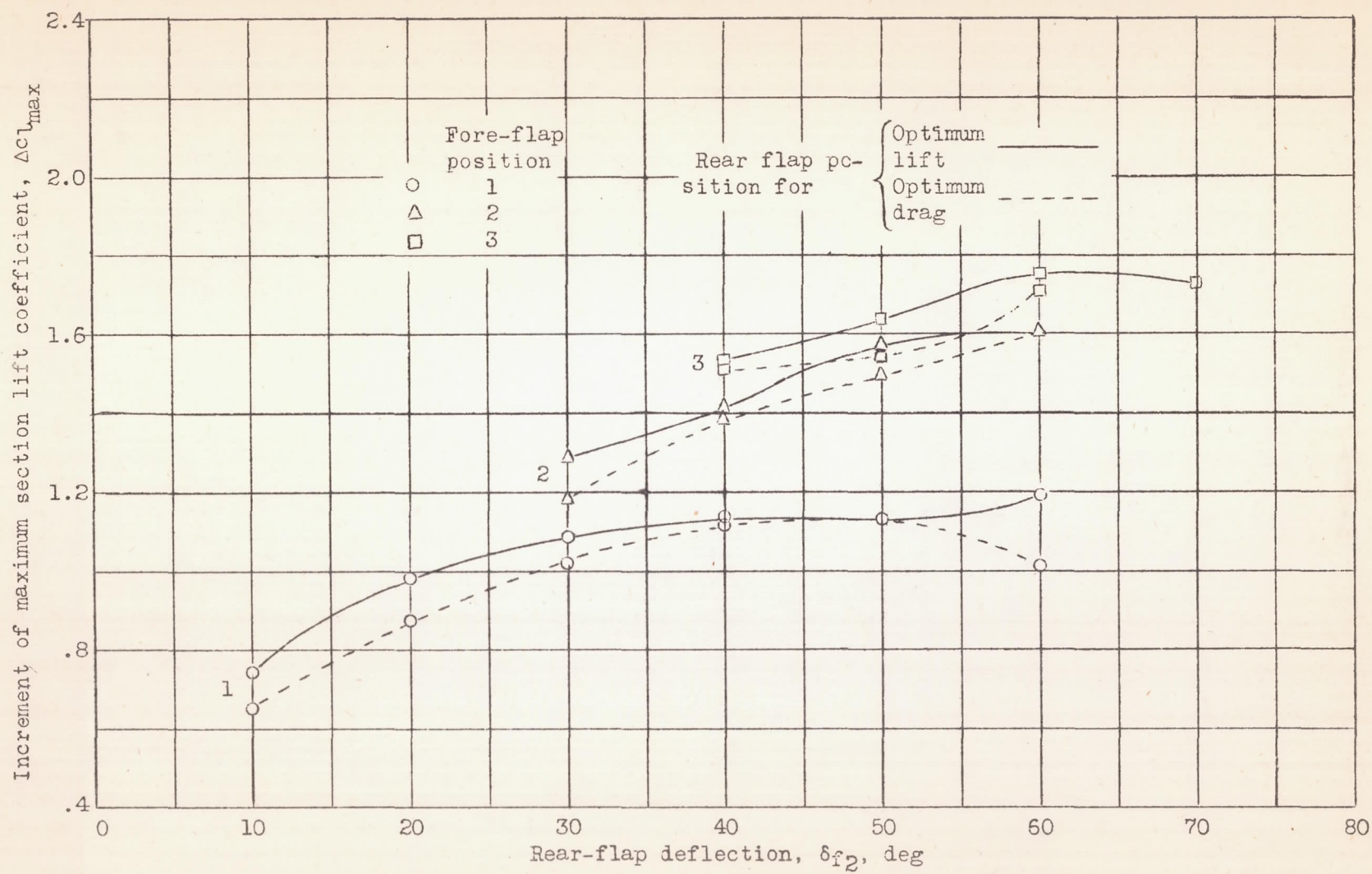
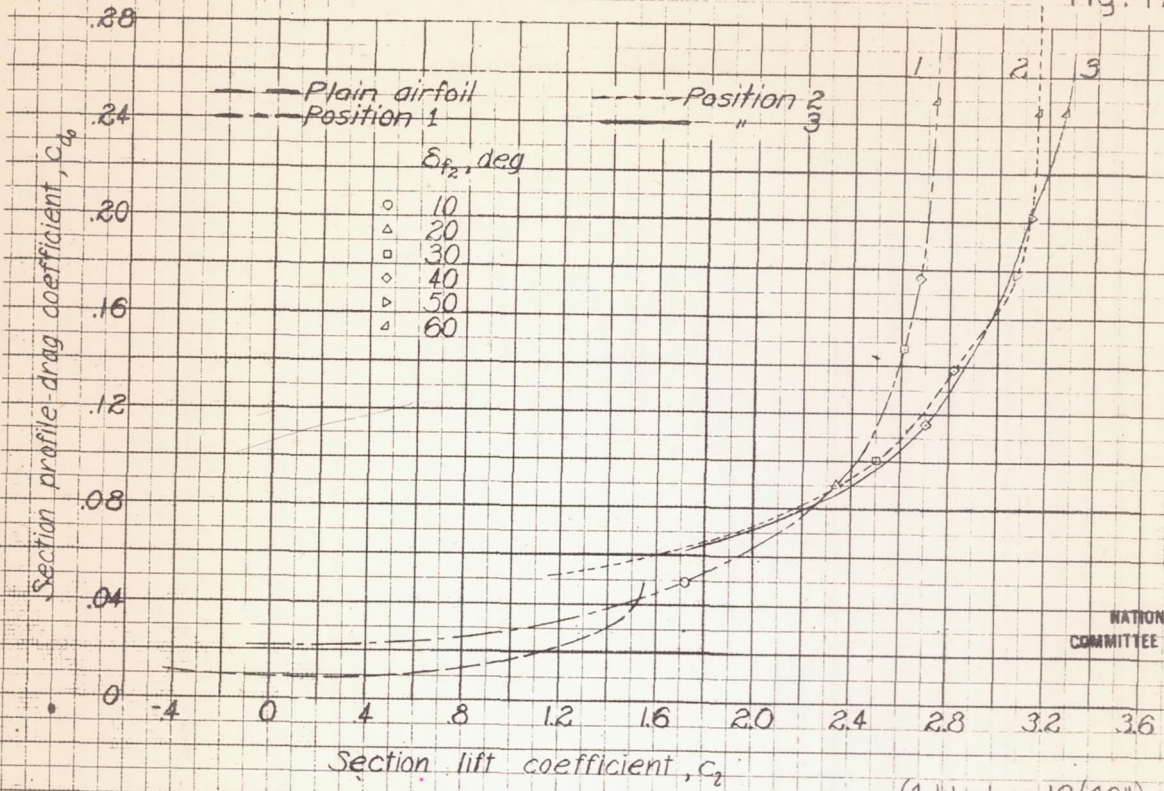


Figure 16.- Effect of rear-flap deflection on the increment of maximum section lift coefficient. The 0.30c double slotted flap on an NACA 23012 airfoil; fore flap A.

394-7

NACA

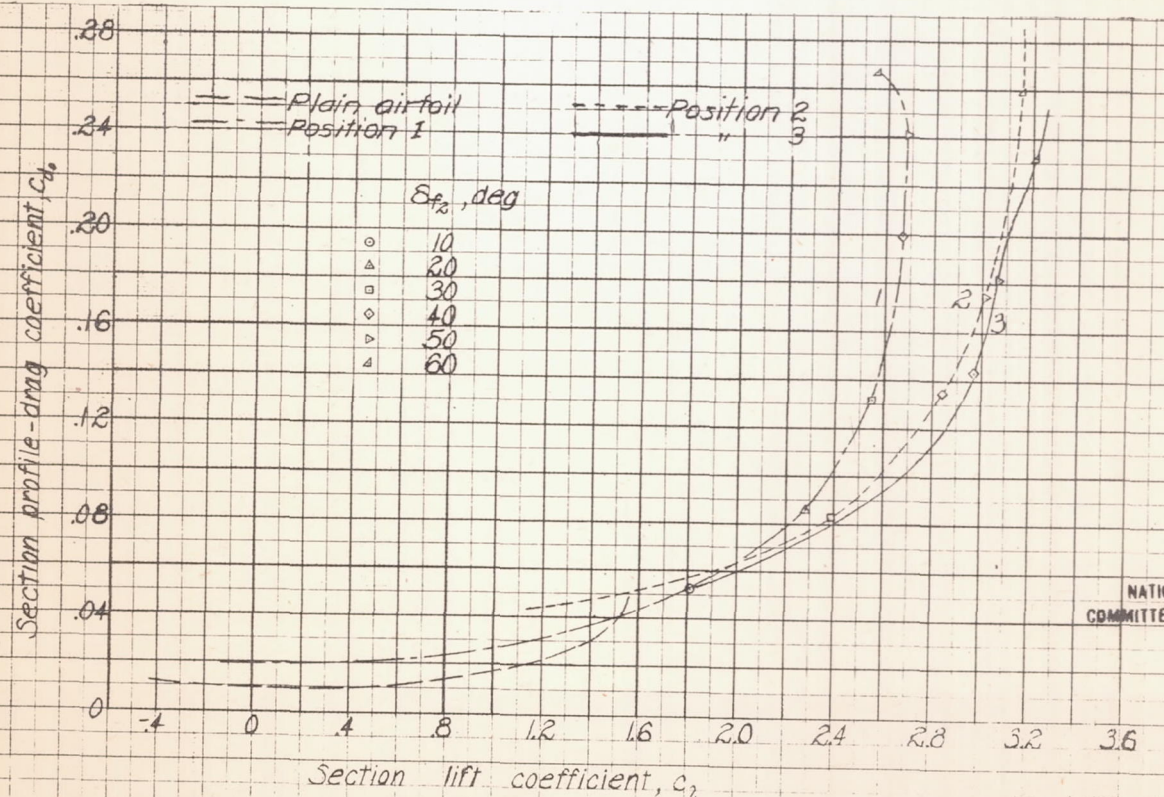
Fig. 17



NATIONAL ADVISORY COMMITTEE FOR AERONAUTICS

(a) Rear-flap positions for $c_{l,max}$

Figure 17.-Profile-drag envelope polar curves for the NACA 23012 airfoil with a 0.30 c double slotted flap. Fore flap A.



NATIONAL ADVISORY COMMITTEE FOR AERONAUTICS

(b) Rear-flap positions for $c_{d,min}$

Figure 17.-Concluded.

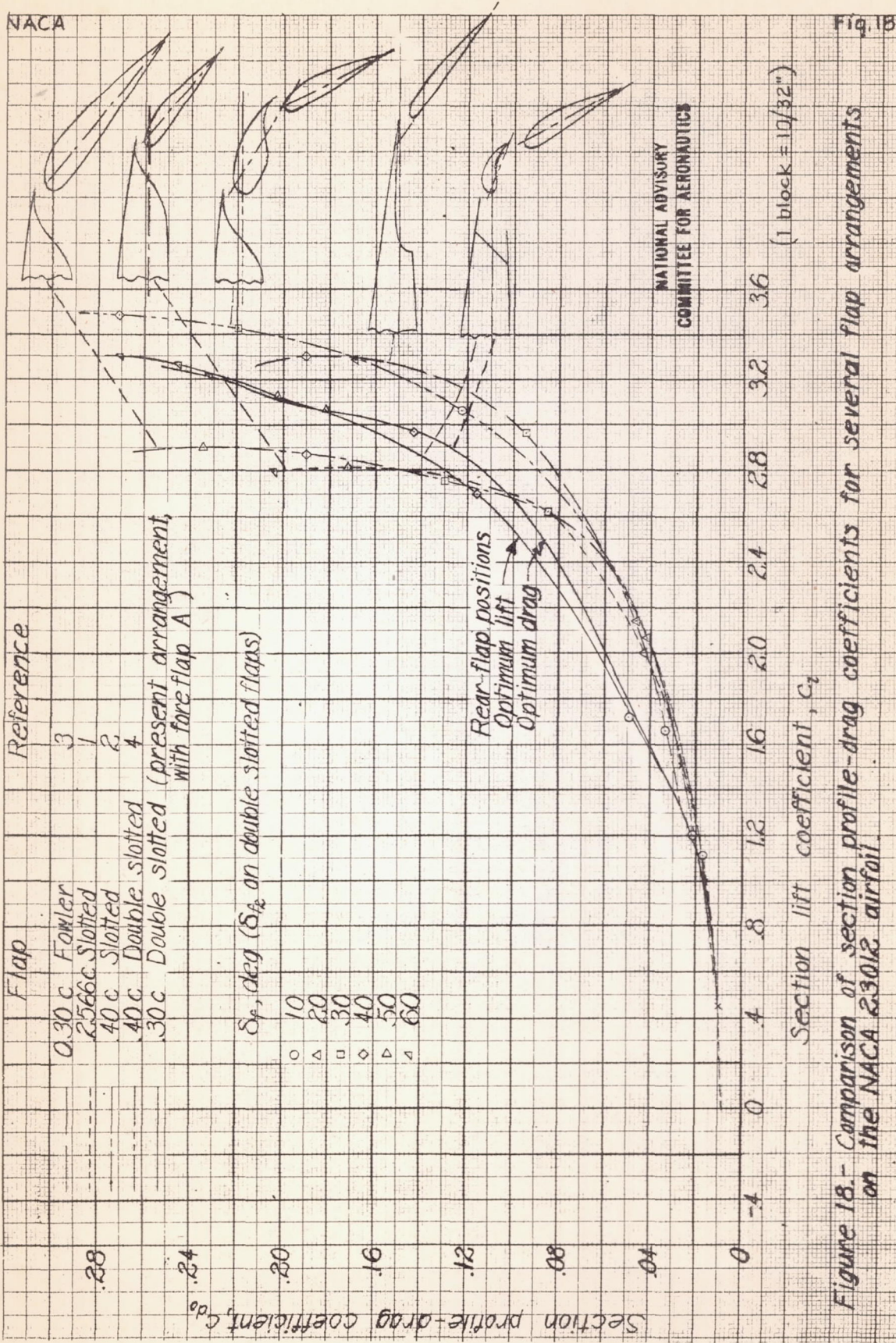


Figure 18.- Comparison of section profile-drag coefficients for several flap arrangements on the NACA 23012 airfoil.

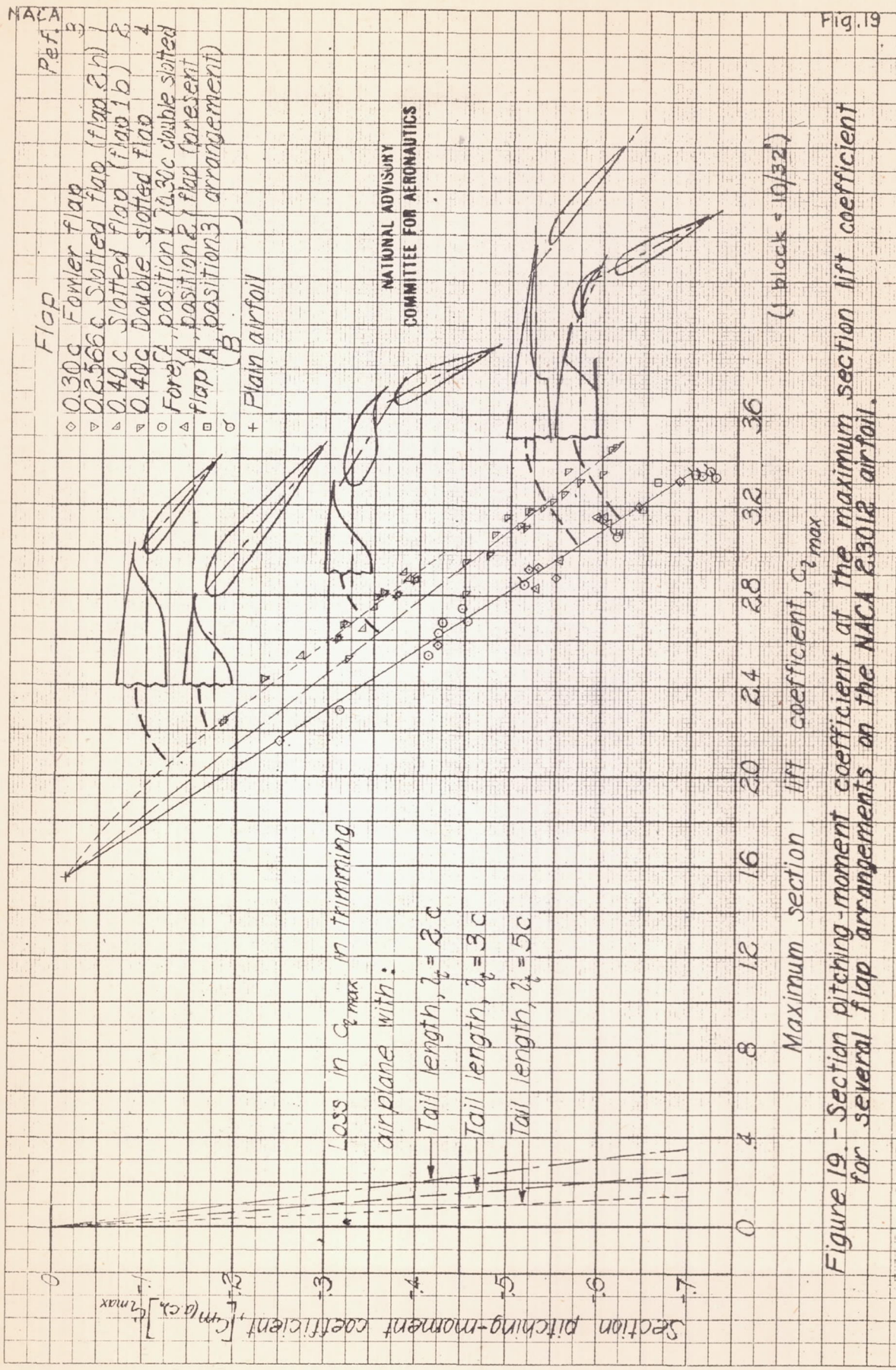


Figure 19. - Section pitching-moment coefficient at the maximum section lift coefficient for several flap arrangements on the NACA 23012 airfoil.

L-469

Fig. 21

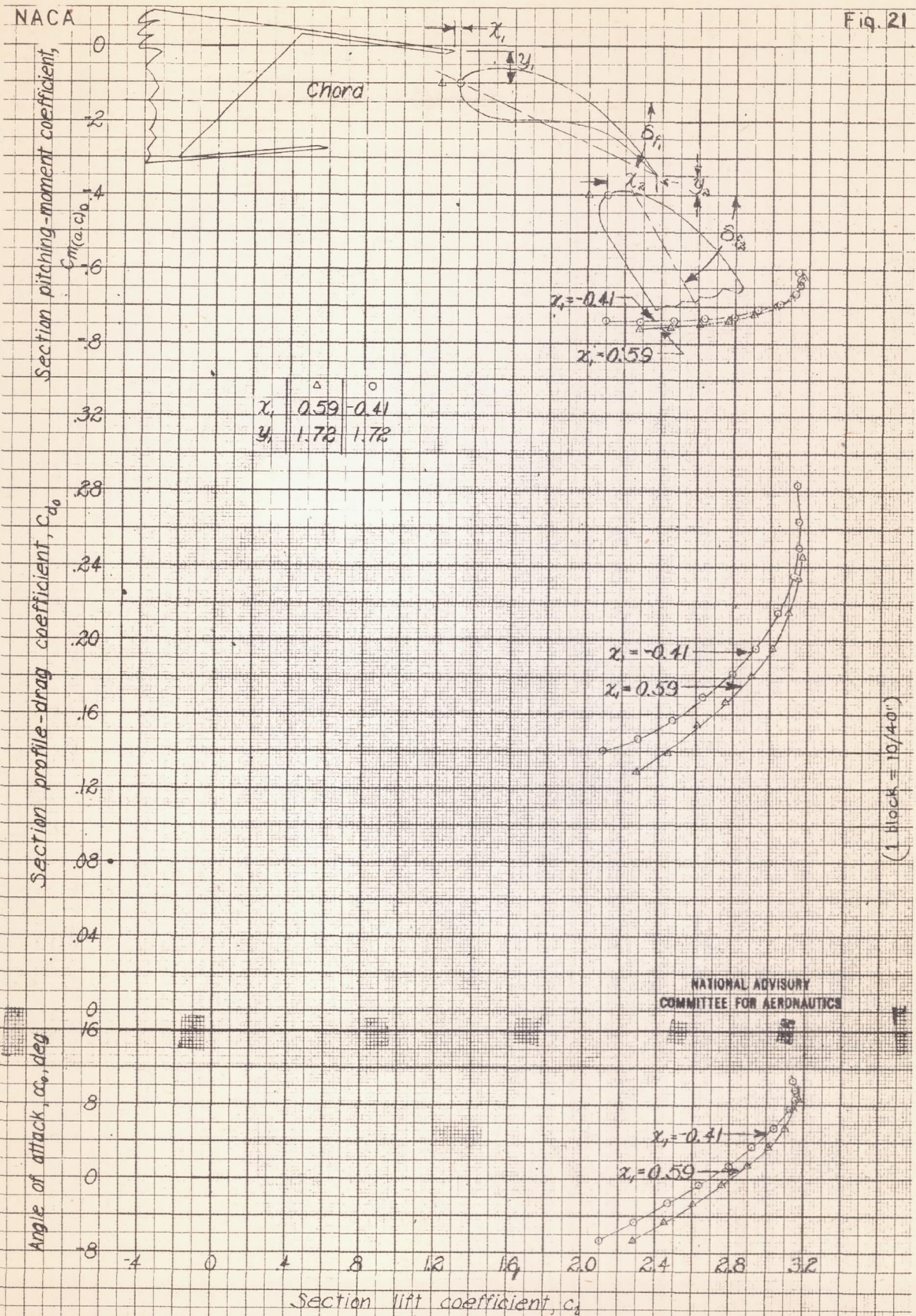


Figure 21 - Aerodynamic section characteristics of the NACA 23012 airfoil with a 0.30c double slotted flap showing the effect of moving the two flaps as a unit parallel to airfoil chord. Fore flap A; $\delta_{f1} = 25^\circ$; $\delta_{f2} = 60^\circ$; $x_2 = 2.60$; $y_2 = 1.05$ (Values of x_1 , y_1 , and x_2 , y_2 are given in percent airfoil chord.)

L-469

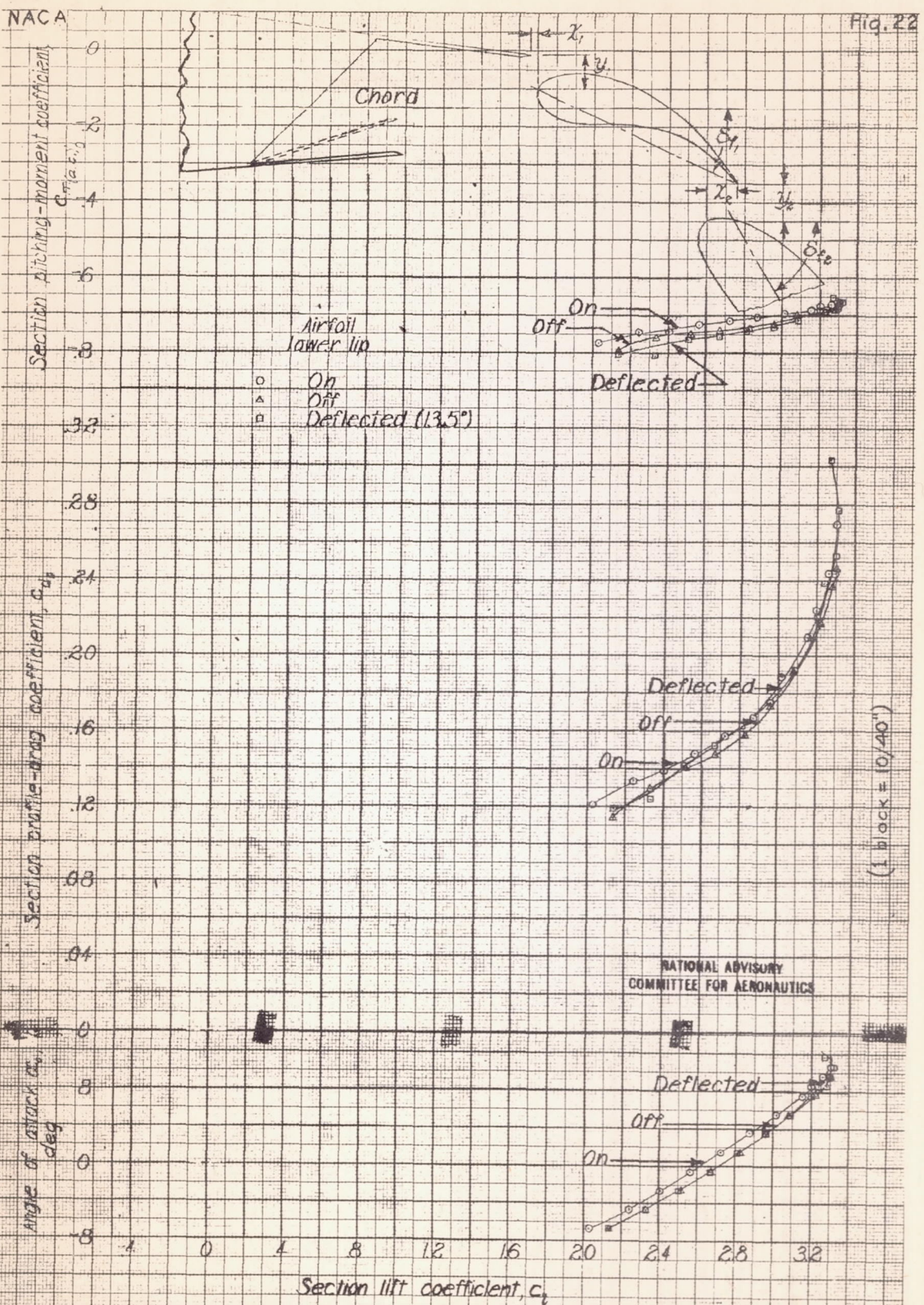


Figure 22. Aerodynamic section characteristics of the NACA 23012 airfoil with a 0.30c double slotted flap showing the effect of the airfoil lower lip. Fore flap A position 3; $\delta_f = 25^\circ$; $x_1 = -0.41$; $y_1 = -1.72$; $\delta_{f2} = 60^\circ$; $x_2 = 1.60$; $y_2 = 2.05$. (Values of x_1 , y_1 , and x_2 , y_2 are given in percent airfoil chord.)

L-469

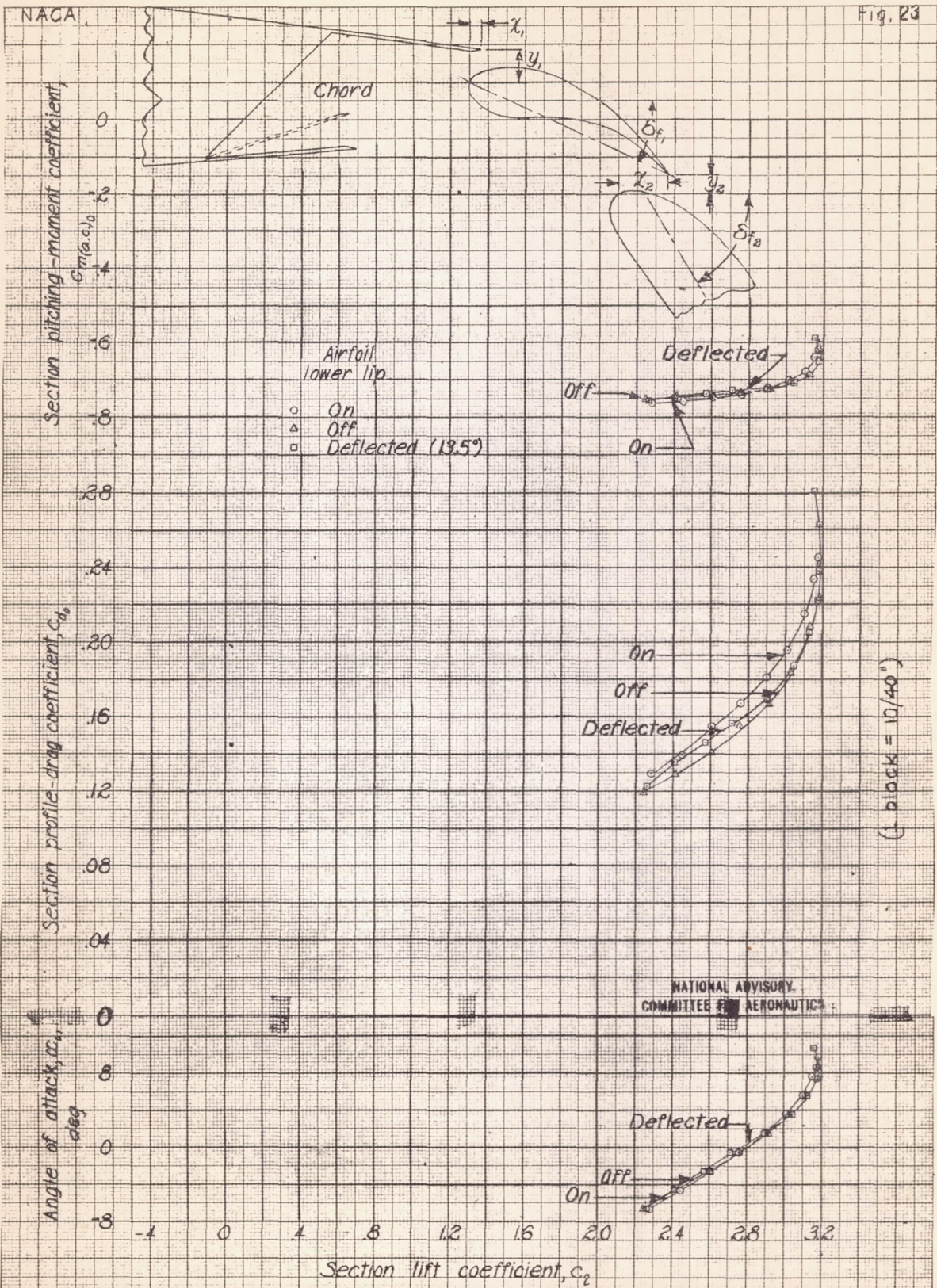


Figure 23.-Aerodynamic section characteristics of the NACA 23012 airfoil with a 0.30c double slotted flap showing the effect of the airfoil lower lip. Fore flap A: $\delta_{f1} = 2.5^\circ$; $x_1 = 0.59$; $y_1 = 1.72$. $\delta_{f2} = 60^\circ$; $x_2 = 2.60$; $y_2 = 1.05$. (Values of x_1 , y_1 , and x_2 , y_2 are given in percent airfoil chord.)

L-489

Fig. 24

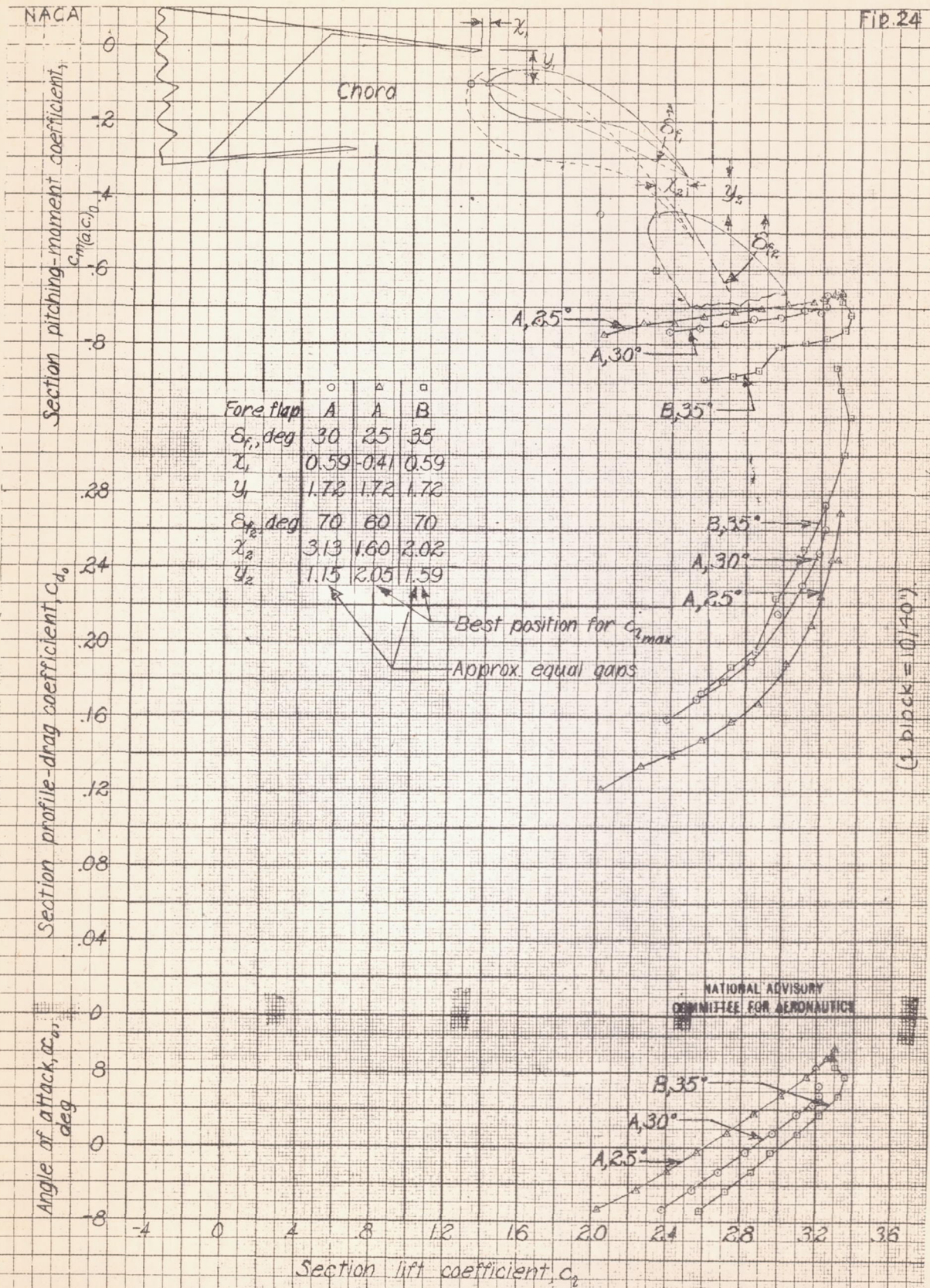


Figure 24.- Aerodynamic section characteristics of the NACA 23012 airfoil with double slatted flaps showing the effect of fore-flap size (Values of x_1, y_1 and x_2, y_2 are given in percent airfoil chord.)